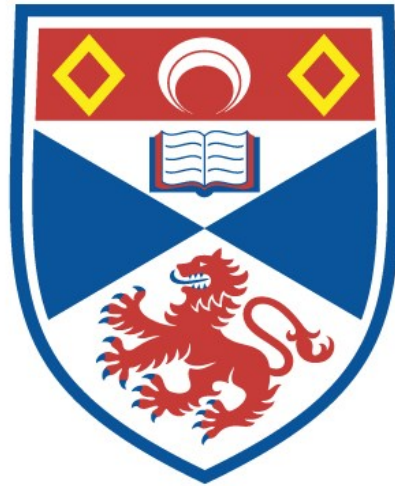


University of St Andrews



Full metadata for this thesis is available in
St Andrews Research Repository
at:

<http://research-repository.st-andrews.ac.uk/>

This thesis is protected by original copyright

**On the Development of an Apparatus
for Low Temperature Measurements of Thermal Expansion.**

**A Thesis
presented by
Thomas Boyter Stewart, B.Sc.
to the
University of St. Andrews
in application for the Degree
of Master of Science.**



DECLARATION

I hereby declare that the following Thesis is based on the results of experiments carried out by me, that the Thesis is my own composition, and that it has not previously been presented for a Higher Degree.

CERTIFICATE

I certify that Thomas Boyter Stewart, B.Sc., has spent not less than four terms as a research student in the Physical Laboratory of the United College of St. Salvator and St. Leonard in the University of St. Andrews, that he has fulfilled the conditions of Ordinance No. XVII of the University Court of St. Andrews and that he is qualified to submit the accompanying Thesis in application for the Degree of Master of Science.

Research Supervisor.

TABLE OF CONTENTS

Section Number.		Page.
I	General Introduction	1
I.I	Introduction	1
I.II	Experimental Methods	5
	(a) X-ray Diffraction	5
	(b) Optical Interference	6
	(c) Optical Lever	8
	(d) Capacitance Dilatation	9
I.III	Object of Thesis	10
II	Apparatus I (Cryogenics)	11
II.I	Requirements	11
II.II	Principle of Method	
	II.1 Production of the Capacity Change	12
	II.2 Measurement of the Capacity Change	13
	II.3 Sensitivity Required	15
II.III	The Dilatometer	16
	III.1 The Case	17
	III.2 The Barrel	18
	III.3 The Specimen Holder	21
	III.4 Size Considerations	22

TABLE OF CONTENTS

Section Number.		Page.
II.IV	Cryostat and Pumping System	23
	IV.1 Heat Losses	24
	IV.2 Construction and Dimensions of Cans	25
	IV.3 Construction of Decks	27
	(a) Top Plate	27
	(b) Top Deck	30
	(c) Lower Deck	32
	IV.4 Heat Switches	34
	(a) Construction	24
	(b) Thermal Contact	36
	(c) Efficiency and Performance	38
	IV.5 Pumping System	39
	IV.6 Temperature Measurement and Control	41
	(a) Measurement	41
	(b) Sensitivity	43
	(c) Calibration	44
	(d) Temperature Control	45
III	Apparatus II (Electronics)	47
III.I	Operating Frequency	47
III.II	Frequency Measurement	48

TABLE OF CONTENTS

Section Number.		Page.
III.II	II.1 R.F. Oscillator	49
	II.2 100 kc/s Oscillator	50
	II.3 5 Mc/s Oscillator	52
	II.4 The Mixer	53
	II.5 Performance	53
III.III	Resonance Detection System	54
	III.1 Principle of the Method	54
	III.2 Electronic Units	57
	(a) L.F. Oscillator and Power Amplifier	58
	(b) Demodulator and N.B. Amplifier	58
	(c) P.S. Detector I	59
	III.3 Power Supplies	59
	III.4 Construction and Mounting of Elec- tronics	60
	III.5 Ferrite Cores	61
IV	Performance of the Apparatus	64
IV.I	Room Temperature Tests	64
	I.1 P.S. Detector II	64
	I.2 Frequency Doubler	65
	I.3 Demodulator and N.B. Amplifier II	65

TABLE OF CONTENTS

Section number.		Page.
IV.II	Sensitivity	66
IV.III	Setting-up Procedure	69
IV.IV	D.C. Magnetisation	72
IV.V	Low Temperature Performance	73
	V.1 Description of a Typical Run	73
	V.2 Results of Runs	76
	(a) Cryostat and Temperature Measurement System	76
	(b) Detection System	77
IV.VI	Conclusions and Recommendations	80

LIST OF ILLUSTRATIONS

Fig.No.		Opp.page.
1	Production of the Capacity Change	12
2	Exploded View of the Dilatometer	16
3	Dilatometer Parts	18
4	Cryostat	23
5	General View of Cryostat and Pumping System	27
6	Layout of Tubing through Decks	28
7	Construction of Coaxial Lines	30
8	Construction of Heat Switches	35
9	Cooling Curves	38
10	The Pumping System	39
11	Temperature Measurement System	42
12	Block Diagram of Electronics	47
13	R.F. Oscillator	49
14	100 kc/s Oscillator	50
15	200 kc/s Receiver	51
16	The Mixer	53
17	Principle of the Method	54
18	L.F. Oscillator and Power Amplifier	57
19	N.B. Amplifier I	58
20	P.S. Detector I	59
21	300 Volt Power Supply	60
22	120 Volt Power Supply	61

LIST OF ILLUSTRATIONS

Fig.No.		Opp.page.
23	General View of Apparatus	64
24	P.S. Detector II	65
25	Frequency Doubler	66
26	N.B. Amplifier II	67
27	Modifications	80

CHAPTER I

GENERAL INTRODUCTION

I.1 Introduction

The importance of low temperature studies of the thermal expansion of solids, towards a better understanding of the equation of state has been amply discussed in literature. Whereas much accurate experimental information of the heat capacity has been obtained down to temperatures $T \sim \theta/100$, there is little corresponding information of the thermal expansion and of the elastic constants. Such information would give an invaluable aid to the study of lattice dynamics and, in particular, the anharmonic nature of the interatomic forces.

The equation of state, for simple solids, was first given by Mie¹ and later, was given a much sounder theoretical basis by Grüneisen² on the assumption of a Debye frequency spectrum. The most general form of Grüneisen's equation is

$$\frac{\alpha}{x} = \frac{\gamma c_v}{v} \quad (1)$$

where x is the isothermal compressibility, c_v is the

2.

specific heat at constant volume and γ is the Grüneisen parameter, which as he pointed out, is approximately constant for many simple solids at average temperatures.

The equation of state can be expressed in the same form as equation (1) on the basis of the Debye theory of specific heats³, where

$$\gamma = - \frac{d \ln \theta}{d \ln v} \quad (2)$$

may be regarded as a measure of the degree of anharmonicity of the lattice vibrations. Although the Debye theory is based on the assumption of harmonic forces in the crystal, which would give $\gamma = 0$ and hence zero thermal expansion⁴, the Grüneisen law was generally taken as correct at low temperatures, because then, only long wavelength acoustical waves are excited and these are just the waves which may be treated as in an elastic continuum having macroscopic elastic constants.

The experiments of Bijl and Pullan⁵ on various solids suggested that there is a breakdown in the rule at temperature $T \sim 0.3 \theta$. Slater⁶ offers a quantitative explanation of an increase in γ on the basis of a variation of Poisson's ratio with volume, but final results of Bijl and Pullan⁷ suggested a decrease in γ at a temperature similar to above.

Barron⁸, in an investigation of the variation of γ ,

based on Born and von Karman lattice dynamics, showed that for a cubic close packed lattice (e.g. copper and aluminium), γ might be expected to have two constant values, a low temperature limit γ_0 , defined by an equivalent temperature θ_0 , and a high temperature limit γ_a , such that $\gamma_a - \gamma_0 \approx 0.3$. He also showed, that the maximum variation of γ between these two limits should occur at temperature $T \sim 0.3 \theta$ agreeing qualitatively with the results of Bijl and Pullan.

The results of Simmons and Balluffi⁹ and Rubin, Altman and Johnston¹⁰, using different experimental methods, indicated that if the variation of γ suggested above does occur, then it does so at a much lower temperature $T \sim \theta/10$ and is not of such large magnitude. (The results show a better quantitative agreement with the theory of Barron as far as magnitude of decrease of γ is concerned.) Because of the disagreement of these results, knowledge of the precise variation of γ is of prime importance.

Since starting this work, published results by Dheer and Surange¹¹ on lead, White¹² on copper and by Abbis et al. and Fraser et al.¹³ on copper and aluminium seem to substantiate the fact that any decrease in γ occurs at the lower temperature and in some cases, e.g. aluminium, there is a tendency for γ to increase. As yet, however, no indication

has been found for γ to tend to the low temperature limit γ_0 . The most recent theoretical approach to this problem by Horton¹⁴ treats the anharmonicity of the lattice waves as resulting from the volume dependence of the elastic constants, and his results for copper agree very well with the experimental data obtained by the workers mentioned in this paragraph.

Of equal interest in the investigations of thermal expansion, is that in metals, the free conduction electrons may also contribute to the thermal expansion as they do to the heat capacity. To estimate this contribution, it is necessary to add to the free energy of the system a further term equal to the free energy of the electrons regarded as a Fermi gas. As shown by Visvanathan¹⁵, this gives as an approximate expression

$$\frac{\alpha}{x} = \frac{1}{v_0} \{ \gamma (c_v)_D + \frac{2}{3} (c_v)_e \} \quad (3)$$

where at low temperatures, $(c_v)_e$ the electronic contribution to the heat capacity is αT and $(c_v)_D$ the lattice contribution is αT^3 . These two become equal for metals at $T \leq \theta/50$ so that the effects of the conduction electrons should become noticeable at around this point. Apart from an anomalous effect noted by White¹² on investigations with iron below 4°K no other apparatus has achieved sufficient sensitivity to study this effect.

I.II Experimental Methods

The oldest method used for measuring thermal expansions, was simply to make a direct measurement of the change in separation of two marks at the ends of a long bar of the specimen material. The need for detailed information, however, discussed in section I.I, caused experimenters to search for some means of obtaining an effective magnification of minute length changes, in an apparatus which would give efficient temperature control over a wide range of temperatures. The experimental methods most commonly used today, can be summarised under the following headings:

- (a) X-ray diffraction
- (b) Optical interference
- (c) Optical lever
- (d) Capacitance dilatation.

The reference authors quoted in each case, are those giving the most accurate results.

(a) X-ray diffraction

X-ray diffraction techniques have been greatly improved over the past few years. A review by Ruhemann¹⁶ in 1937 indicated that till that time, an accuracy of 1 part in 10^4 had not been achieved, whereas Simmons and Balluffi⁹ in 1957 quote an accuracy of 1 part in 10^7 . The main

advantages of this method seem to be (1) that the measurements are absolute, i.e. it gives a direct measure of the lattice expansion and (2) only the specimen is at the low temperatures, so that appreciable errors do not arise due to thermal gradients in the apparatus. No X-ray method to date, however, has been capable of detecting the extremely small dilatations that occur at $T < \theta/30$. Simmons and Balluffi were unable to detect any change in the lattice constants of copper below 25°K and state in fact, that below 40°K their experimental errors are relatively large ($> 5\%$).

It has been suggested¹⁷, that differences might be expected in data obtained from X-ray measurements and from those measurements utilising massive polycrystalline specimens. This has in fact been shown to be true at high temperatures ($T \approx$ melting point)¹⁸, but the excellent agreement of the results referred to above with those of Rubin, Altman and Johnston¹⁰ indicate that this anomaly does not arise at low temperatures if sufficiently pure specimens are used.

(b) Optical interference

The method, which was first used by Fizeau¹⁹, involves the measurement of the displacement of an interference fringe pattern derived from two glass plates whose

separation is controlled by the specimen length. Originally, the separation was obtained from the difference in height of the specimen and a reference material, but in general, measurements are made absolute by placing the specimen directly between the plates, usually in the form of three rods of equal length^{10, 20}.

Rubin et al. using this method claim to detect a length change of 1.5×10^{-7} cms. In a more recent attempt, Fraser and Hallet¹³ obtain a Fabry-Perot type of interference pattern and although no information is given as regards accuracy, this method appears inferior to that previously noted.

New techniques in cryostat construction, make this method applicable to the lowest temperatures. The only obvious disadvantages appear to be the restriction placed on the sensitivity by the use of extremely short specimens and the localised heating effects of the powerful light beams required.

It is of interest to note, that in the work of Rubin et al., it was found impossible to detect any difference between single crystal copper and polycrystalline copper that was oxygen free.

(c) Optical lever

In this method, small relative length changes are magnified by the deflection of a beam of light either by prisms or by mirrors, the apparatus being calibrated to give dilatations as a function of the angle of deflection of the light beam. The majority of experiments carried out using this principle have made use of some reference material^{21, 22}, but the method has been made absolute by Huzan et al.²³ by comparing the length changes of a specimen relative to a control specimen of the same material. The authors quote as an ultimate sensitivity, the detection of a length change of about 30 \AA of a 5 cm. specimen.

The main inaccuracies in the results, using this method, would appear to arise from the fact that temperature equilibrium state measurements are not taken (i.e. a dynamic method is used) giving rise to thermal gradients in the system.

The optical lever principle has been used by Jones²⁴ in an infra-red detector. Using a photoelectric amplifier, the system is capable of detecting a length change of about 10^{-12} cms. The suspension system is not directly applicable to low temperature thermal expansion work, but even taking into account a loss in sensitivity due to suitable modification, the detection system would seem to offer a great

improvement over methods previously used.

(d) Capacitance dilatation

In order to construct an apparatus which would eliminate the need for long light paths in the cryostat and as a result make temperature control much more efficient, Bijl and Pullan⁵ utilised the principle that the capacity of a parallel plate condenser is strongly dependent on the separation of the plates. A capacitor was constructed such that the separation of the plates is controlled by the length of the specimen and the entire unit or dilatometer was cooled through the required range of temperature.

This method has been adopted by Dheer and Surange¹¹ and by White¹². The first two mentioned, calibrated the changes in length (i.e. capacity) against the change of frequency of an oscillator having the dilatometer as the capacitive element of the L.C. tank circuit, whilst the other (viz. White) makes an accurate bridge measurement determination of the actual change in capacity of the condenser.

This method, unlike the others, cannot be made absolute, but very accurate calibration can be applied, and the sensitivity achieved is very much better than by any of the other methods. For instance, White claims to detect a length change of $1 \overset{\circ}{\text{A}}$ in a specimen of length ~ 5 cms. and hopes to improve this by a factor of 10.

I.III Object of thesis

Because of the uncertainty noted in section I.I regarding the temperature dependence of the Grüneisen ' γ ' (at the time of starting this work, the results of White, Abbiss et al. and Fraser et al., had not been published), it was decided to try to develop an apparatus (a) of sufficient sensitivity and accuracy to check previous experimental data and (b) to work in a temperature range where it would be possible to study the effect of the conduction electrons in metals.

From considerations of the methods previously adopted, and the facilities available, it was decided that the most suitable approach would be a refinement of the capacitance dilatometer method of Bijl and Pullan. This type of measurement can be made very sensitive to small relative length changes or dilatations ($\delta l/l$ of a specimen), although, as will be shown later, (section IV.III) great sensitivity in detection of a change need not necessarily imply great accuracy in the final results.

It is the object of this thesis to show the development of the apparatus to its present state, starting from a few basic requirements, indicating the principles involved at each stage and showing how most of the initial defects were eliminated.

CHAPTER II

APPARATUS I (CRYOGENICS)

This chapter is devoted to the cryogenic section of the apparatus, including the capacitance dilatometer. A rough indication of the basic requirements of the apparatus as a whole is followed by a detailed description of the component parts, which are considered under the following headings:

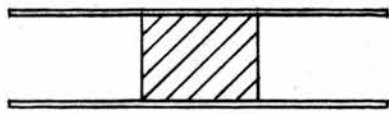
- (1) Dilatometer
- (2) Cryostat and Pumping system
- (3) Temperature measurement and control.

II.1 Requirements

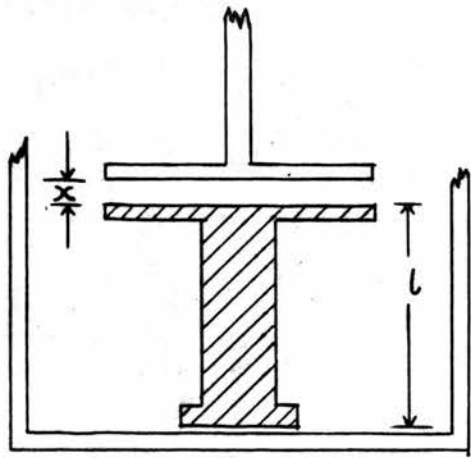
(a) The system as a whole must be sufficiently sensitive to detect and measure a dilatation of $\leq 0.5 \times 10^{-7}$, in order to compare favourably with other workers.

(b) As the method is not absolute, the calibration should be accurate enough to support the above sensitivity.

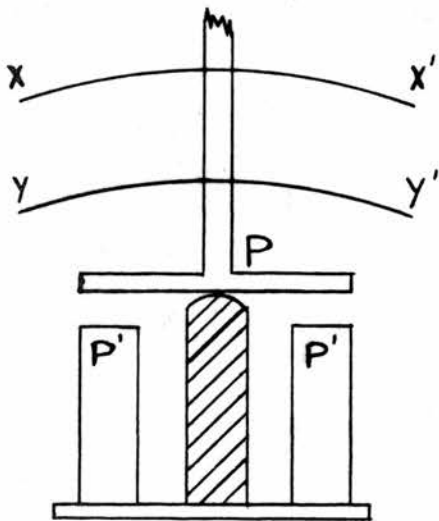
(c) The cryostat should be constructed such that any desired temperature in the range considered can be maintained within prescribed limits.



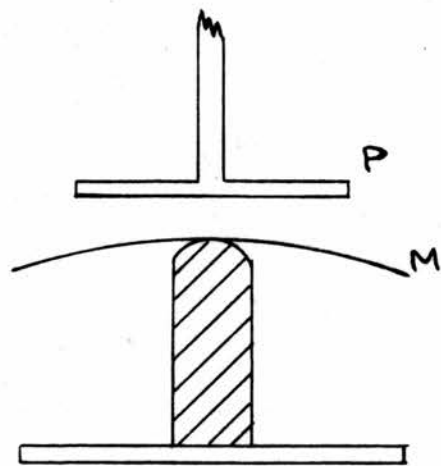
a



b



c



d

Fig. No. 1.
Production of the Capacity Change.

(d) Any spurious effects inherent in the apparatus should be small and completely reproducible so that they can be eliminated by dummy experiments.

(e) As it is necessary to replace the specimen fairly frequently, it would be very advantageous to carry out this procedure without seriously interfering with the remainder of the apparatus.

(f) The apparatus as a whole, in particular the cryostat, should be mechanically robust and not subject to microphonics (due to pumps etc.).

II.II Principle of the Method

II.II.1 Production of the Capacity Change

Fig. I (a and b) illustrates two methods for the conversion of length changes to capacity changes. Neglecting practical difficulties of both methods, the advantage of the second of these is the substantial effective magnification of a dilatation, i.e. a dilatation $\delta l/l$ of the specimen gives a relative gap change of the condenser $\delta l/x$ which is a magnification of l/x . It was preferred, however, to have a more flexible system whereby less restriction is placed on the shape of the specimen. This is done by using two constrained metallic plates as the condenser, one being fixed, and the other controlled by keeping it in contact

with the specimen. To overcome the difficulty of a low mechanical resistance moving system, which would retain its properties at low temperatures, it was decided to use a flexed membrane M (Fig.1.d) as the moving plate. Although, as far as is know, this method has not been used at low temperatures for dilatation work, the principle of utilising changes in the shape of a diaphragm or membrane to give capacitive changes has been extensively used for electrical pressure measurements^{25, 26}. In addition, as will be shown later (section II.III.3), this system allows for a simple interchange of specimens.

The system is not absolute, due to areal changes in the plates and length changes in the supports as the temperature is altered. This, however, is not really a serious disadvantage, as it is possible to calibrate the system against these changes.

II.II.2 Measurement of the Capacity Change

As this apparatus is a development of the system used by Bijl and Pullan, a brief summary of the causes of the major inaccuracies in their results is given before indicating how it was intended to overcome them. These workers placed the dilatometer condenser in the tank circuit of an R.F. oscillator, and measured a change in

length of a specimen as a change in frequency of the oscillator. The three main defects were

(1) The final accuracy of the results was limited by the long term stability of the R.F. oscillator.

(2) Because the inductance coil was immersed in the different coolant liquids required to cover the temperature range, (i.e. oxygen and hydrogen) the inductance value 'L' was dependent on the liquid used and varied with bubbles in the liquid.

(3) As shown in Fig.1.c, the live plate of the dilatometer condenser P' was the lower plate. The value of stray capacity of the coaxial leads from this plate to the inductance coil was about 50% of the condenser capacity and was found to vary with the temperature of the dilatometer.

In the present system, the dilatometer condenser is used as the capacitive element of a parallel resonant L.C. circuit. The inductance, which is positioned on the top deck (Fig. 4) of the cryostat, and so always under the same conditions of temperature and pressure, is loosely coupled to the output of an R.F. oscillator. The relative change in length between the specimen and the copper supports can be calculated from the change in resonant frequency of the tank circuit after calibration. The

measurements can be made virtually absolute by comparing the copper with diamond, which has a very much smaller thermal expansion than copper. The accuracy of the results is therefore determined by the sensitivity of the resonance detection, and by the short term stability of the R.F. oscillator, i.e. the oscillator need be stable only for a period of time long enough to make the necessary measurements.

II.II.3 Sensitivity required

It is probably worth while at this stage, to indicate the sensitivity required of the resonance detection system. The resonant frequency of the tank circuit is approximately

$$V_0^2 = \frac{1}{4\pi^2 L(E + c)}$$

where E is the stray earth capacity.

$$\therefore dV_0 = -\frac{1}{2} V_0 \frac{dc}{(c + E)}$$

$$\text{assuming } dE = 0$$

if the capacity of a parallel plate condenser is taken as

$$c = \frac{A}{4\pi x}$$

$$\text{then } dc = -c \frac{dx}{x} = -c \frac{dl}{x}$$

where $dl = l \times (\text{dilatation})$

$$\therefore dV_0 = \frac{1}{2} V_0 \frac{c}{(c + E)} \frac{1}{x} \times (\text{dilatation}). \quad (4)$$

Assuming a dilatation of 0.5×10^{-7} and anticipating the values of x , l and V_0 to be 0.2 mm., 2 cms and 5×10^6 c/s respectively.

$$dV_0 \doteq 10 \times \frac{c}{(c + E)} \text{ c/s.}$$

The stray capacity contribution E comes mainly from the lead connecting the condenser to the inductance. The dilatometer was designed to reduce this contribution to negligible proportions ($< 1/50 c$) by making the top plate of the condenser P the live plate so that the lead to the inductance could be as short as possible. Thus, to detect a dilatation of 0.5×10^{-7} it must be possible to measure the resonant frequency to within 10 c/s off resonance.

II.III The Dilatometer

The principles effecting the design of the dilatometer have been discussed in the preceding paragraphs and can be roughly listed as

- 1) relatively compact and robust
- 2) top plate of condenser as the live plate
- 3) simple interchange of specimens
- 4) little restriction on shape of the specimens.

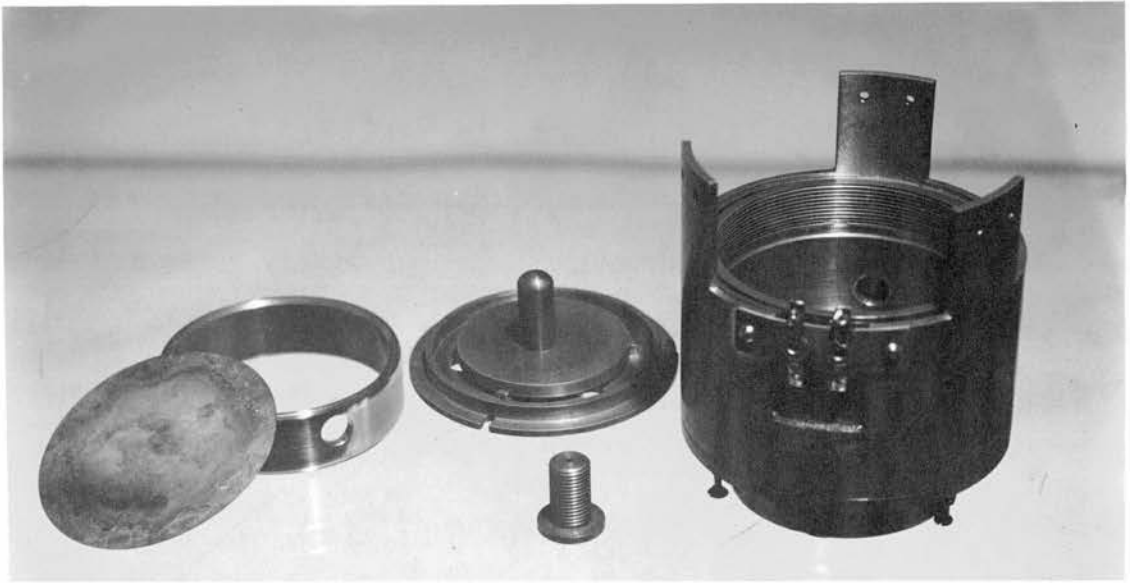
Opposite (Fig.2) is an exploded view, to scale, of the actual unit. The whole, apart from the insulating quartz disk Q and the brass locking nut N , was machined from \wedge

a single piece of high grade copper, to reduce the risk of introducing strain effects which might otherwise occur in the cooling process. The dilatometer itself may be considered as being comprised of three parts, the case, the barrel and the specimen holder.

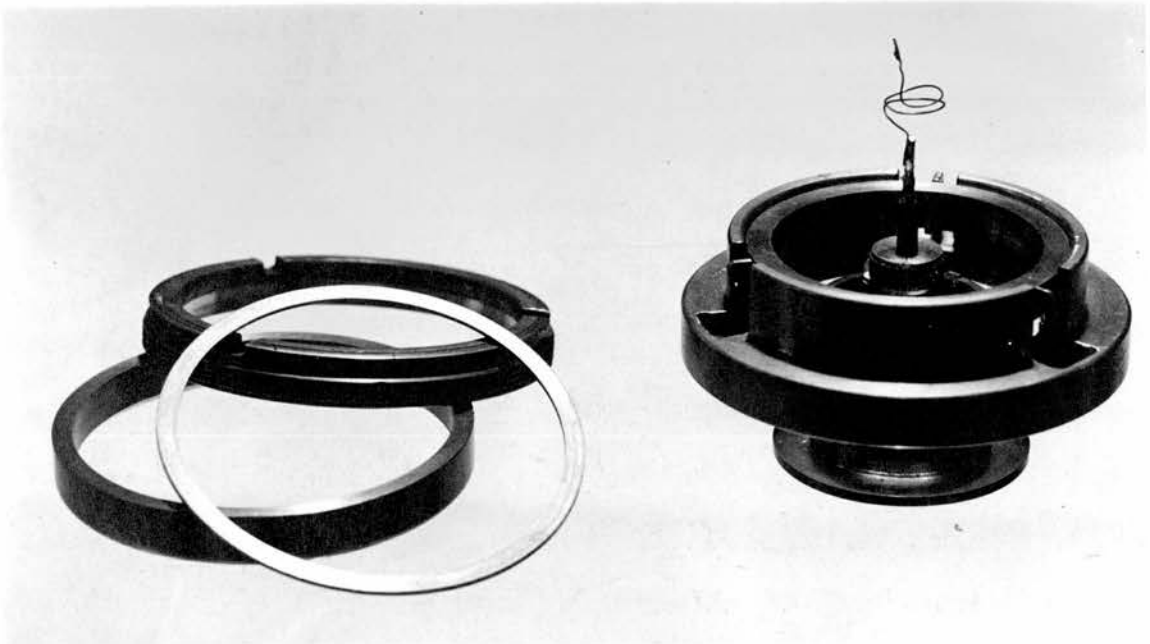
II.III.1 The Case

The main purpose of the case is to support the rest of the dilatometer when it is in position inside the cryostat, and to act as a housing for the platinum resistance thermometer. In order to solder the electrical connection (at point X) between the dilatometer condenser and the inductance (also to reduce weight) the case is cut away as much as possible, leaving three lugs to connect the dilatometer to a flange on the underside of the lower deck of the cryostat (Photo - Fig.4). This provides a very firm support for the dilatometer and allows for ease of dismantling, when necessary, to make minor modifications. The case is connected to the barrel by three 6 B.A. screws set equidistantly around the circumference of the lower end. As can be seen from the drawing, it is possible to remove the barrel while retaining the case in position, but in practice it is simpler to disconnect them as a whole.

The drawing shows the copper former, on which the



(a)



(b)

Fig. No. 3.
Dilatometer Parts.

resistance thermometer is wound, in position inside the case. A rectangular portion of the case was cut away and a strip of insulating material with two metal bus bars was bolted across the space. (Photo - Fig.3a). After positioning the former, the ends of the thermometer wire were soldered to the bus bars. With this arrangement, there is no need to disturb the thermometer, even when dismantling the dilatometer.

II.III.2 The Barrel

As shown in the drawing, this part contains both plates of the condenser. For this reason, it was essential that it be machined to a very high degree of accuracy, and a tolerance of better than .001 cm. was placed on all important dimensions. The barrel is constructed in such a way as to make assembly quick and easy, whilst to fulfil the original requirements the live plate of the condenser is the top plate.

It is of great importance that the membrane be mounted in as strain-free a manner as possible to minimise any warp effects that might occur with temperature change. Since, however, the membrane is the earthed plate of the condenser, there is no need to isolate it from the barrel, and it is clamped, uniformly, rigidly and at a constant radius over the whole of its periphery, between a shoulder

in the barrel and a knife edged annular distance ring. The membrane is of 4 thou phosphor bronze sheet which was annealed in a nitrogen atmosphere to eliminate strains which might have arisen in machining.

Phosphor bronze seemed to be the most suitable choice of material for the membrane, since experiments to date (Bijl and Pullan) seem to indicate that it retains its elastic properties even after repeated coolings to low temperatures. A further advantage of using this material is that the expansion coefficient of phosphor bronze is almost exactly equal to that of copper, so that on cooling, there should be no tendency for the plate to buckle or stretch due to differential expansion. The best check on the validity of the above statements is in the reproducibility of the results. This is discussed in section IV.V.2.b when giving experimental results.

When assembling the barrel, the membrane M and knife edged distance piece D are placed in position, the top plate of the condenser P with its suspension can then be assembled as shown in Fig.2 and lowered as a unit into the barrel to sit on the top knife edge of the distance piece D. A second annular ring D' with a knife edge on the lower face is then placed on top of this, and the whole is rigidly clamped with a washer W and the brass locking nut N.

Details of the top plate assembly are given in the drawing and so only a few explanatory notes are necessary. As required, the plate is insulated by supporting it from the quartz disk Q. The central rod of the plate passes through a clearing hole in the centre of the quartz disk and the two pieces are kept in contact by the spring and locking nut A. The plate is held inside the barrel by the support S at a predetermined distance (~ 0.2 mm.) from the membrane. This construction ensures that the condenser gap (i.e. the distance between the membrane and the plate P) is effected when cooled, only by the contraction of a length of copper equal to the separation of the plates. The retaining piece R is incorporated as a precaution against movement of the plate and disk relative to the support. Three small phosphor bronze springs B are used to clamp the quartz disk in position, these are permanently secured to the support at one end and have a steel pin connected to the other for fitting to the retaining ring. The photograph (Fig.3.b) shows the top plate assembly with a brass jig, which is used to ensure that the quartz disk and hence the condenser plate, are centrally situated with respect to the barrel.

The three copper pieces which are in contact with the quartz disk (i.e. P, S, R) are ground to leave only three

small pips (~ 1 mm. square) as the points of contact in order to minimise the effects of differential expansion. Pips also proved to be extremely useful when minor length changes were required, as it was possible to remove small amounts from each pip and still retain a very high degree of parallelism. This would have been much more difficult with a continuous surface. Another important feature, are the holes drilled through the wall of the barrel and the knife edged distance piece (photo - Fig.3.a). There are two 3/8 in. diameter holes to ensure, when pumping, that there is no pressure difference across the membrane which might lead to a false curvature.

II.III.3 The Specimen Holder

The specimen holder is composed of three parts, the distance piece E, the base plate F and the base G. The drawing also shows the position of a specimen Sp. The difference in lengths of the specimen and distance piece imparts some curvature to the membrane. This curvature must be sufficient so that at no time during a run is the specimen separated from the membrane, otherwise the capacity of the condenser is not governed by the length of the specimen. The springs B' which keep the specimen holder in position are strong enough to counteract the downwards pressure from the curved membrane applied to the base via

the specimen.

A specimen is easily replaced by simply releasing the three springs and removing the specimen holder. To mount a new specimen, a brass plug (photo - Fig.3.a) is screwed into the threaded boss of the base, and a short glass rod is then pushed through the central hole of this plug and into a blind hole in the base of the specimen. With the rod still in position, the specimen holder is raised onto the shoulder of the barrel and clamped by the springs. The glass rod and brass plug are then withdrawn leaving the specimen held in position by the slight downward pressure of the curved membrane. The process of replacing a specimen, therefore, does not disturb any other part of the dilatometer. Equally important, is the fact that the specimen shape is relatively unrestricted. The tolerance on the length is $\pm .02$ mm., and the diameter is unimportant, the only requirement being that the top end is rounded.

II.III.4 Size considerations

The dilatometer could have been made more compact by a reduction in length of the top plate of the condenser, i.e. a shorter distance between the quartz disk Q and the face of the plate. It was preferred to leave sufficient space for modification should it prove necessary at a later stage to load the membrane in some way to ensure contact

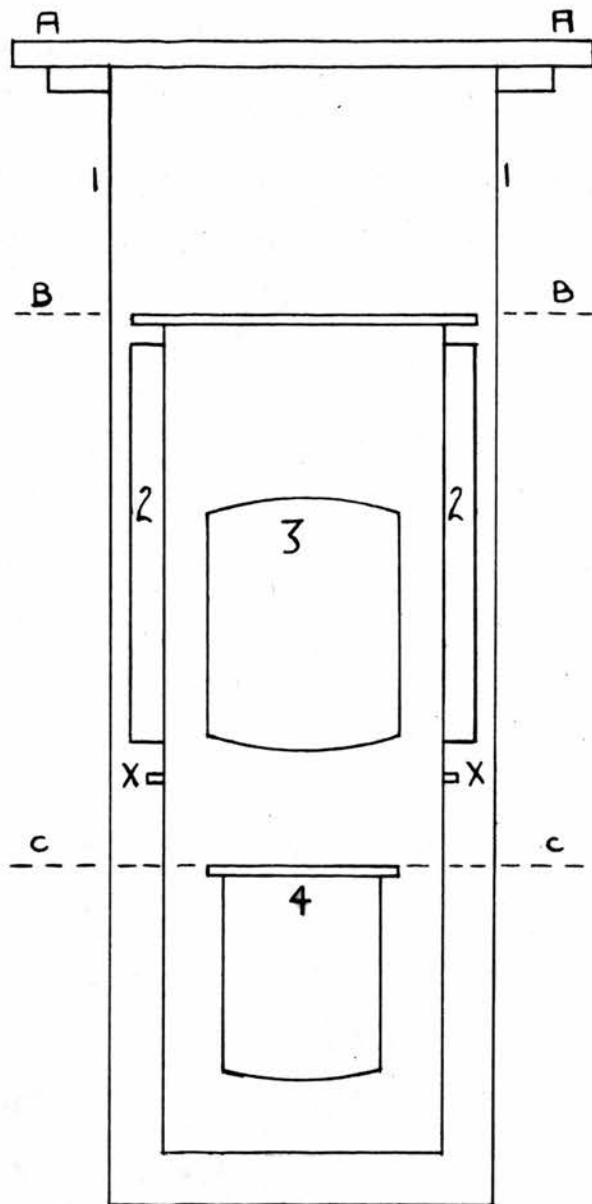


Fig. No. 4.

Cryostat.

(Photograph taken with
outer can and lower
part of radiation
shield removed.)

with the specimen. The massiveness of the dilatometer may be regarded as a drawback as far as cooling time is concerned (section II.IV.4.c) but this disadvantage is offset by the fact that a sudden small heat influx does not alter the temperature appreciably. A rough calculation shows that at $\sim 150^{\circ}\text{K}$, 1 joule of heat would alter the integrated temperature of the dilatometer by only $.05^{\circ}\text{K}$. Since the maximum value of the cold leak to the dilatometer from the surroundings is approximately 3.3 watts, the chance of there being a sudden influx of 1 joule is extremely remote. The temperature of the dilatometer can therefore be held constant for long periods of time without much difficulty.

II.IV Cryostat and Pumping System

In order to obtain the degree of accuracy required, it must be possible to bring the dilatometer to any intermediate temperature in the range considered and to hold this temperature constant for a period long enough to make the necessary measurements. As the apparatus is intended to operate ultimately down to liquid helium temperatures, it was decided that a metal cryostat would be easier to construct and more wieldy in use than very large glass dewars. The cryostat essentially consists of three airtight containers surrounded by a large can (1) which

is continuously pumped to give a thermal vacuum ($\sim 10^{-6}$ mm. Hg). The three cans (Fig.4) contain (2) liquid oxygen or nitrogen, (3) liquid hydrogen or helium, and (4) the dilatometer, all of which can be thermally linked by two mechanical heat switches to bring the temperature of the dilatometer to the required point.

Shown in the drawing, are three deck levels which, for description purposes, will be designated as: A-A the top plate, B-B the top deck and C-C the lower deck. The relative spacing of these three decks is governed by consideration of the conduction heat losses through the pumping and filling tubes.

II.IV.1 Heat Losses

When designing the cryostat, a compromise had to be made between overall length of the cryostat, and conduction heat losses to the cold sinks. For the purpose of calculation, it was assumed that the vacuum inside the outer can is good enough to reduce conduction and convection losses due to gas in the cryostat to negligible proportions with respect to radiation losses and conduction losses through the tubes.

In estimating the heat losses to the nitrogen can, a rate of loss of liquid nitrogen equal to 250 cc./hour was

taken as a reasonable value. The major contribution to this loss, $i \frac{S}{\lambda}$ from radiation from the outer can and only a quarter of the total heat influx is through the pumping tubes. There was therefore no need to make the distance between the top plate and the top deck excessively large, leaving more space for the other two cans.

The hydrogen can is subject to a total heat influx from three sources: 1. radiation heating from the nitrogen can, 2. conduction from the top deck and 3. conduction from the lower deck. The third of these arises from the electrical heating required to control the temperature of the dilatometer. This contribution can become significant in the extreme cases (i.e. when the dilatometer is at liquid nitrogen temperatures with hydrogen in can 3 and when the dilatometer is at hydrogen temperatures with helium in can 3), but is neglected in the estimated values quoted. These are a loss of liquid hydrogen at the rate of about 2 c.c./hour and of liquid helium at about 100 c.c./hour.

II.IV.2 Construction and Dimensions of the Cans

The outer can is made from 10 gauge brass with an outer diameter of 7 ins. and an overall length of 29 ins. The top end is soldered to a heavy brass flange which is slotted to accommodate a standard 8 in. diameter "O-type" gaco seal and is bolted tightly against the top plate with

eight symmetrically placed studs screwed into the top plate. The total weight of can and flange (32 lbs) is such that it was necessary to add counterweights over pulleys to help lift the can into position without damaging the rest of the cryostat.

The outer wall of the concentric liquid nitrogen can is of 16 gauge brass with an outer diameter of 6 ins. and the inner wall is of 13 gauge copper with an outer diameter of 5 ins. The can is closed at the ends by two brass flanges at a distance of 11 ins. giving a capacity of approximately 1.25 litres. To reduce heat losses to the dilatometer from the outer can, the inner wall is extended below the level of the liquid nitrogen can to form a radiation shield which can be detached at point X to give access to the dilatometer can.

The hydrogen container is made from 16 gauge copper with an outer diameter of 4 ins. and an all over length of 8 ins. giving a capacity of 1.5 litres. The ends of the can are made from 16 gauge sheet copper and are spun to lessen the chance of pressure collapse.

The dilatometer can is also made from 16 gauge copper with an outer diameter of 3.1/2 ins. and a length of 5 ins. The bottom end is closed with a spinning, but as this can has to be removed to allow access to the dilatometer, it

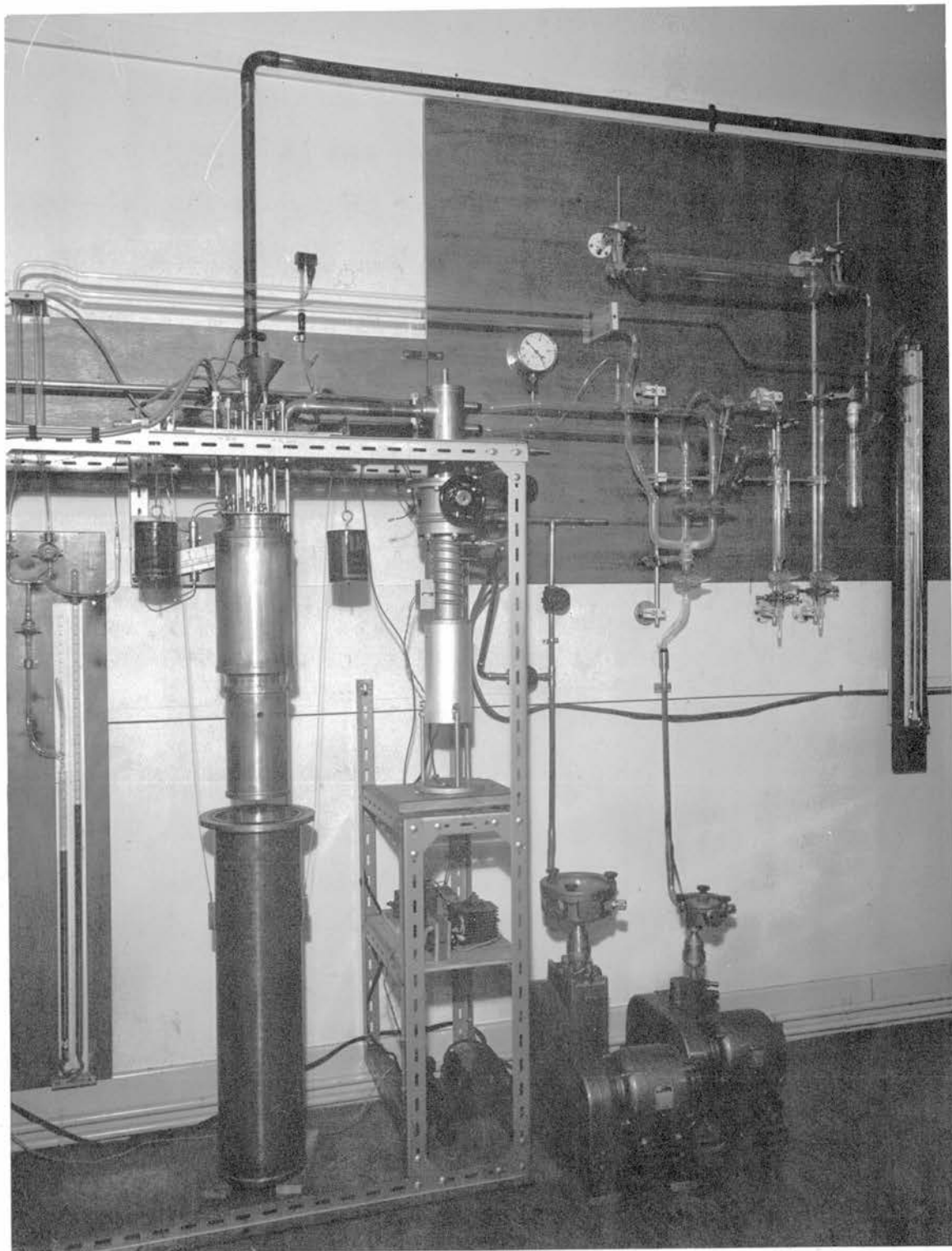


Fig. No. 5.
General view of Cryostat and Pumping System.

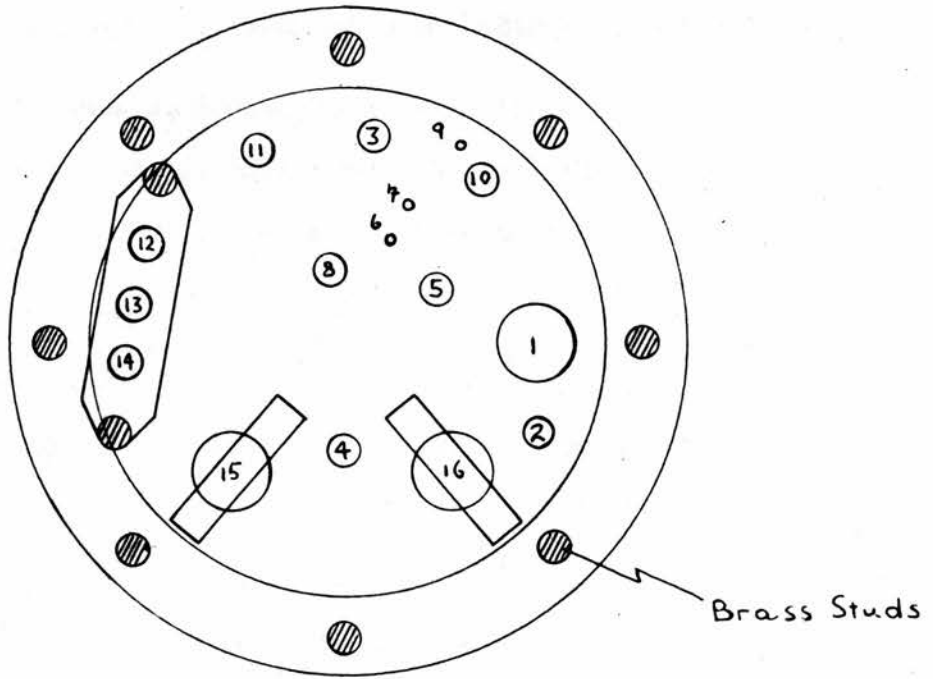
was necessary to incorporate a vacuum seal on the top end. A flange is soldered to this top end and is slotted to accommodate a closed ring of 1/16 in. diameter indium wire (the slot is 1/16 in. wide to a depth of 1/32 in.). The flange is screwed tightly into position against the lower deck with eight symmetrically placed 4 B.A. screws.

II.IV.3 Construction of the Decks

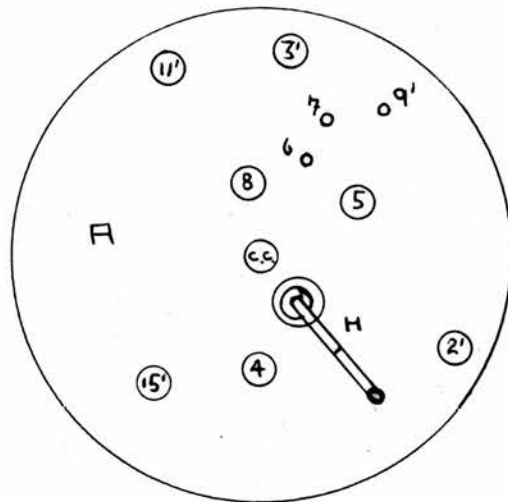
The descriptions which follow show that each deck is used both as a support for those parts of the cryostat which hang below, and as a rigid anchoring point for auxiliary parts of the apparatus such as heat switches etc.

(a) Top Plate

The top plate has to withstand quite a high degree of stress in supporting the rest of the cryostat and especially when tightening the nuts which hold the outer can in position. Any tendency to deformation would ruin the vacuum seal. It was, therefore, necessary to use heavy gauge brass sheet in the construction and the final dimensions of the plate are $12.1/2 \times 9 \times 3/8$ ins. This plate is supported at a height of 5 feet from the floor on a rigid 'Handy Angle' framework which allows easy access to the cryostat (photo - Fig.5). An approximately scaled drawing of the top plate is given in Fig.6.a., showing the relative positions of the various tubes and electrical leads and



(a) Top Plate



(b) Top Deck

Fig. No. 6.
Layout of Tubing through Decks.

also of the brass studs used to support the outer can.

All tubes passing down the cryostat are of thin walled German silver to reduce conduction losses. The list below corresponds to the numbered tubes in the drawing.

1. Outer can pumping line: the diffusion pump connection is made through a bellows, to reduce microphonics, into a 1 in. 'Ideal' brass elbow soldered straight onto the top plate.

2, 3. Liquid nitrogen can, filling and exhaust tubes: as it is unnecessary to pump the liquid nitrogen can, both connections are open ended, standard centimetre tubing, protruding 1.1/2 ins. above the plate. A funnel is used when filling.

4. Liquid hydrogen (or helium) filling tube: a 7/16 B.S.F. fitting is soldered to the top of an 8 mm. line to accommodate a transfer tube used for filling. Approximately 9 ins. below the top plate, the tube diameter is reduced to 4 mm. to lessen the chance of oscillation in the can when helium is used as coolant.

5. Hydrogen return line: a standard centimetre tube is connected through a bellows to the hydrogen return line. Provision is also made for pumping this can and details are given when discussing the pumping system.

6, 7. Level indicator: two lengths of capillary

tubing are soldered into the hydrogen can, one to the top of the can and the other to the bottom. These two are then connected to a butyl phthalate "differential pressure" level indicator.

8. Dilatometer pumping line: a T-junction is soldered on top of a length of centimetre tubing from the dilatometer can. The horizontal arm of the T is led to the pumping system via a metal bellows and the vertical connection is made to a "sow", which is used to connect the leads from the resistance thermometer to the temperature measurement system. This pumping tube is also used to allow a few centimetres of helium exchange gas into the can.

The "sow" is fabricated by soldering six kovar seals onto a small plate which, in turn, is soldered to the top of a small can. In this way, the electrical leads are kept separate while giving a compact vacuum-tight seal.

9. Vapour pressure thermometer lead: this is a length of capillary tubing from a small reservoir on the lower deck to a mercury manometer.

10. Vacuum Gauge: a penning gauge head was mounted directly onto the top plate, but for reasons discussed in section IV.IV, this was discarded in favour of a pirani gauge. This is sufficiently sensitive as only an indication of pressure and not an absolute value is required.

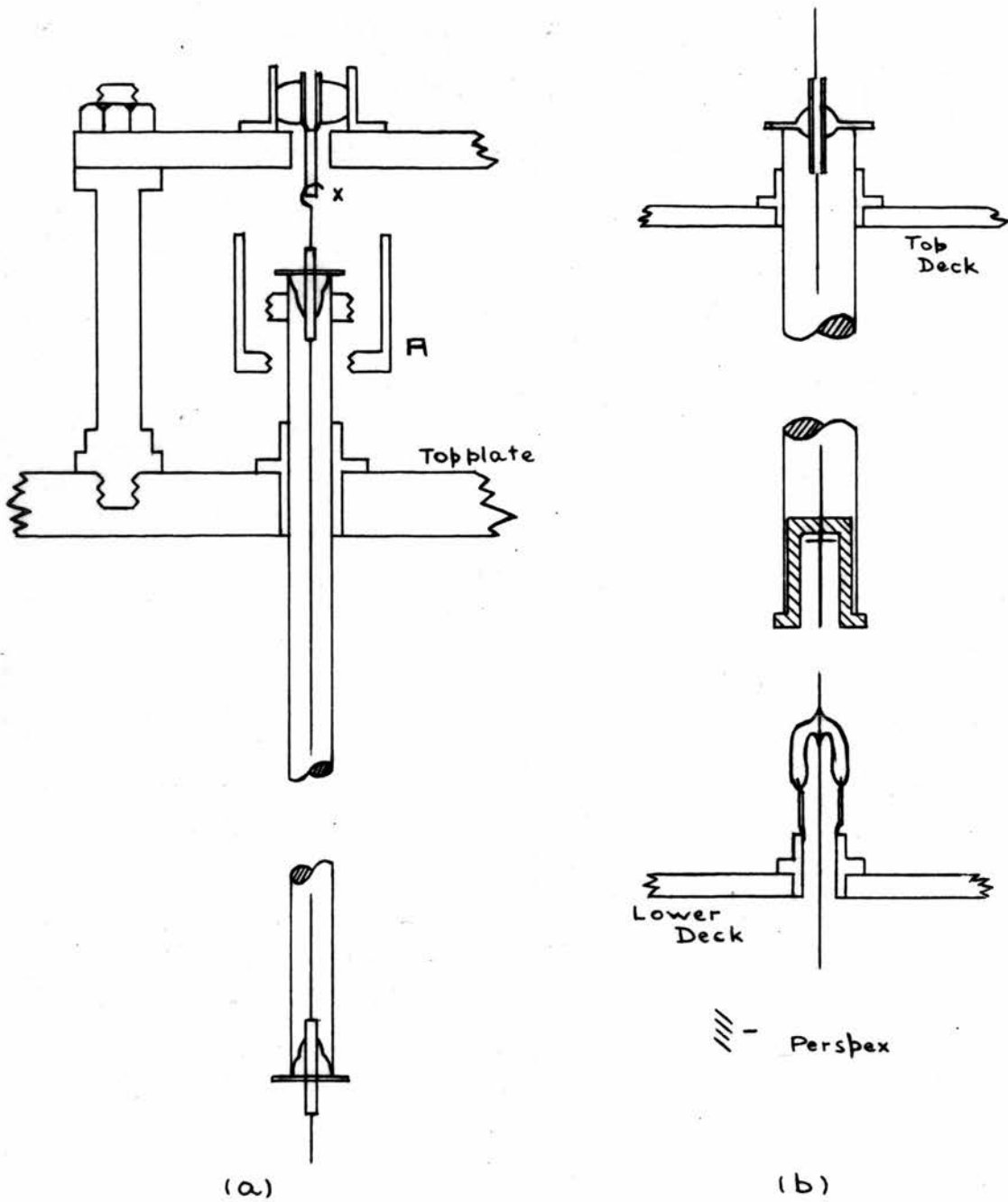


Fig. No. 7.
Construction of Coaxial Lines.

11. Sow for heater leads: the leads from the heaters on the dilatometer can and the hydrogen can (used for boiling off excess liquid) are led through a short length of centimetre tubing to another six pin sow.

12, 13, 14. Electrical leads to L.C. tank circuit: the construction of the leads is shown in Fig.7.a. A simple coaxial line is made by stretching 36 gauge eureka wire between two kovar seals soldered onto the ends of a length of 8 mm. tubing. This tube is 'Woods metallised' into position on the top plate stretching from 1 in. above the top plate to 1.1/2 ins. above the top deck. The connections to the electronics are made through 'Belling Lee' coaxial sockets screwed onto a strip of 3/16 in. brass and rigidly supported 2.1/2 ins. off the top plate. After soldering the wire from the top seal to the socket at X, the coaxial line is completed by screwing piece A into position. This construction eliminates any direct pick-up between the three leads and reduces the risk of accidental damage to the soldered connections.

15, 16. Heat switches: the construction of the heat switches is discussed fully in section II.IV.4.

(b) Top Deck

The top deck, situated 6 ins. below the top plate, is 6.1/2 ins. in diameter and was machined from a piece

of 3/8 in. brass plate. This plate is thermally anchored to the liquid nitrogen container to act as a cold spot for the pumping lines etc. As can be seen from the schematic drawing of the cryostat (Fig.4.b), it was impracticable to mount the deck and the can as a unit as this would have interfered with the mounting of the hydrogen can. For this reason, the top deck was machined with a flange on the underside to which the nitrogen can could be bolted after assembling the cryostat (see Note at the end of section (c)).

The layout of tubes through the top deck is shown in Fig.6.b. The asymmetry was contrived to leave sufficient space for mounting both the inductance coil of the L.C. tank circuit (at A) and the first heat switch (at H) which connects the nitrogen can to the hydrogen can. The numbers on the drawing correspond to the numbered tubes on the top plate and for these, no more explanation is necessary, except that the dashed numbers imply clearing holes.

The only additional tube to pass through this deck is the central coaxial line c.c. connecting the dilatometer condenser to the inductance. This line, which terminates 3/4 in. above the top deck and passes down through the hydrogen can is constructed as in Fig.7.b.

A kovar seal is soldered onto the top end of the length of centimetre tubing and a piece of 24 gauge eureka wire pushed down through the seal and the tube. The bottom end is threaded through the perspex plug and soldered, a few inches from the end, to a small washer. The wire at the top is then pulled up taut, bringing the plug into position against the bottom end of the tube, and soldered to the kovar seal. This construction is used in preference to a second kovar seal because, being close to the dilatometer, this lower end is subject to slight variations of temperature which might cause a kovar seal to change its electrical properties.

(c) Lower Deck

The lower deck, which was machined from brass plate, is 4 ins. in diameter and is 0.2 in. thick. To fulfil its primary purpose, this deck is flanged and drilled to support the dilatometer case and the dilatometer can. The hydrogen can is positioned between the top and lower decks which are 17 ins. apart.

The hydrogen can is supported by the tubing which passes through the top deck, but as only one of these (tube No.8) is continued to the dilatometer can, it was necessary to use a "spider" arrangement to support the lower deck rigidly enough to anchor the second heat switch.

Also mounted on this deck are (1) a glass to copper seal (Fig.7.b) to make the electrical connection between the central coaxial line and the live plate of the dilatometer condenser and (2) a small cylindrical can which is the reservoir for the vapour pressure thermometer.

Spider supports are commonly used in assembling metal cryostats and liquefiers to align the component parts before soldering permanently into position. Three lengths of 4 mm. German silver tubing were soldered at both ends to short pieces of 6 B.A. screwed wire and symmetrically connected to the lower deck. This unit was then raised into position under the three limbed spider, which is soldered onto the lower protruding end of the central coaxial line, and screwed firmly into place.

Note: The nitrogen can was mounted after assembling the rest of the cryostat. To simplify this operation, and to allow for removal of the can, if necessary, the filling and exhaust tubes (2, 3) were constructed in two parts. The top portion is permanently soldered to the top plate and protrudes approximately 3 ins. from the underside. The lower part is permanently connected to the liquid nitrogen can, but is hand soldered to a sleeve at the upper end. When the can is raised and bolted to the top deck, the sleeve fits the upper portion of the tube and

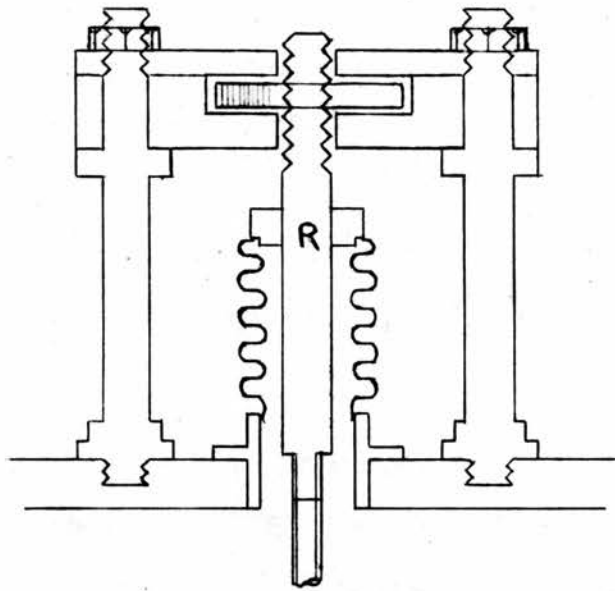
is soft soldered into position. If necessary to remove this can, therefore, no heat, which might cause pressure leaks in neighbouring soldered joints, need be applied to the top plate.

II.IV.4 Heat switches

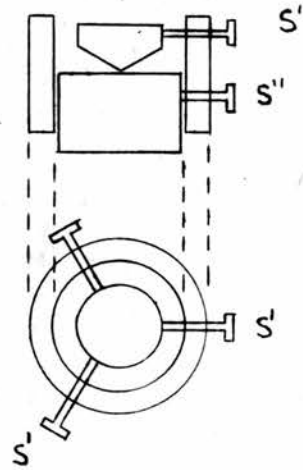
The cryostat requires two heat switches to connect the cold sinks to the dilatometer. Mechanical switches were thought to be more practicable than helium exchange gas switches because of space limitations within the cryostat. In recent years, many workers have applied the technique of using mechanical thermal switches instead of helium exchange gas for cooling purposes in the design of cryostats for specific heat measurements²⁷.

(a) Construction

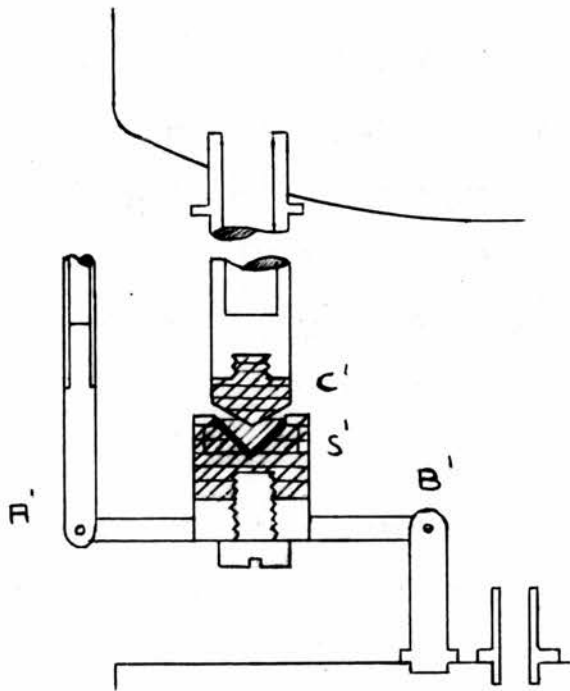
The main factor influencing the design of the switch itself was that one of the actuating rods from the top plate has to pass through the narrow annular gap between the nitrogen and hydrogen cans. As this gap is only $3/8$ in. wide, it places a restriction on the lateral displacement of the rod. The simple lever arrangement, used for both switches, fulfils this condition very well, since a vertical displacement of $1/4$ in. which is more than enough to break thermal contact, gives rise to a lateral displacement of approximately $1/32$ in.



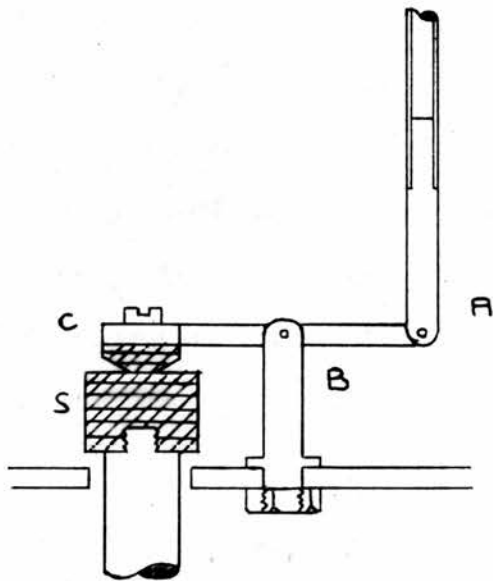
(a)



(b)



(c)



(d)

Fig. No. 8.
Construction of Heat Switches.

As shown in the drawing (Fig.8), the two switches are of slightly different construction, although in both cases thermal contact is made through a copper cone and socket fitting. The switching action is such that the actuating rod is under tension when the switch is closing, i.e. when the maximum force is required.

The first switch (Fig.8.d.), situated on the top deck is used to make thermal contact between the radiation shield and the hydrogen can. The actuating rod A, the fulcrum B and the contact cone C, are all bolted to the lever arm for ease of removal. To give a better thermal contact between the deck and the switch, one end of a copper braid is anchored to the deck, and the other is soldered to a thin copperspade terminal which is tightly jammed between the contact cone and the arm of the lever. The socket is screw fitted onto a long 1/2 in. diameter copper rod which passes through a clearing hole in the top deck and is soldered onto the hydrogen can.

The second switch (Fig.8.c), situated on the lower deck, gives thermal contact between the hydrogen and dilatometer cans. The arrangement is only slightly different from above in that the fulcrum is at the end of the lever arm at B' and the socket is screw connected to the middle of the arm at S'. A copper braid is again jammed against

the socket to improve thermal contact. The cone is screw fitted onto a copper rod which is soldered into the bottom of the hydrogen can. This copper rod is drilled out as shown, to allow the coolant liquid to come as close as possible to the point of contact of the switch.

The requirements for the controlling mechanism are (1) that it must be vacuum tight and (2) that it must be capable of exerting a reasonable tensile force. The arrangement shown in Fig.8.a is used for both switches. Since the vertical movement is small (not greater than 1/4 in.) it was felt that a flexible bellows system could be used with little risk of metal fatigue and subsequent leaks. The 4 mm. German silver actuating tube is connected at the upper end to a brass rod (R) which is brought from the vacuum system through the bellows to the screw arrangement used for raising and lowering the rod. The second requirement is fulfilled by using a very fine thread (40 t.p.i.) on the brass rod.

(b) Thermal Contact

The sockets of the heat switches are faced with a thin layer of indium metal to give a large area of contact between socket and cone. Manchester²⁷ achieved a 75% reduction in cooling times by using a copper-indium contact as opposed to a copper-copper contact. The problem of

obtaining this thin layer, however, proved slightly troublesome.

The first attempt was made by simply melting indium metal into the socket, and closing the switch. Although the metal is very soft at room temperatures, it was not possible to make a deep enough impression, leaving a very thick layer of indium. A slight improvement was obtained by using the tool, which was made for machining the socket, to remove excess indium. This process, however, seemed to have the effect of work hardening the indium and left a smooth hard surface onto which it was impossible to get a good impression of the cone.

Fig.8.b illustrates the method finally adopted to get both a good impression of the cone, and a reasonably thin layer of indium (~ 1 mm.). Indium metal is melted into the socket and machined as before to leave a thin layer on the surface of contact. Cone and socket are then mounted in the jig, with the cone firmly anchored by the three screws S' and the socket free to move vertically. On applying heat to the jig, the indium melts allowing the cone to sink into position inside the socket and pushing out excess indium. Cone and socket can then be held in this position by tightening screw S'' and the heat switch firmly assembled. The operation is completed by removal

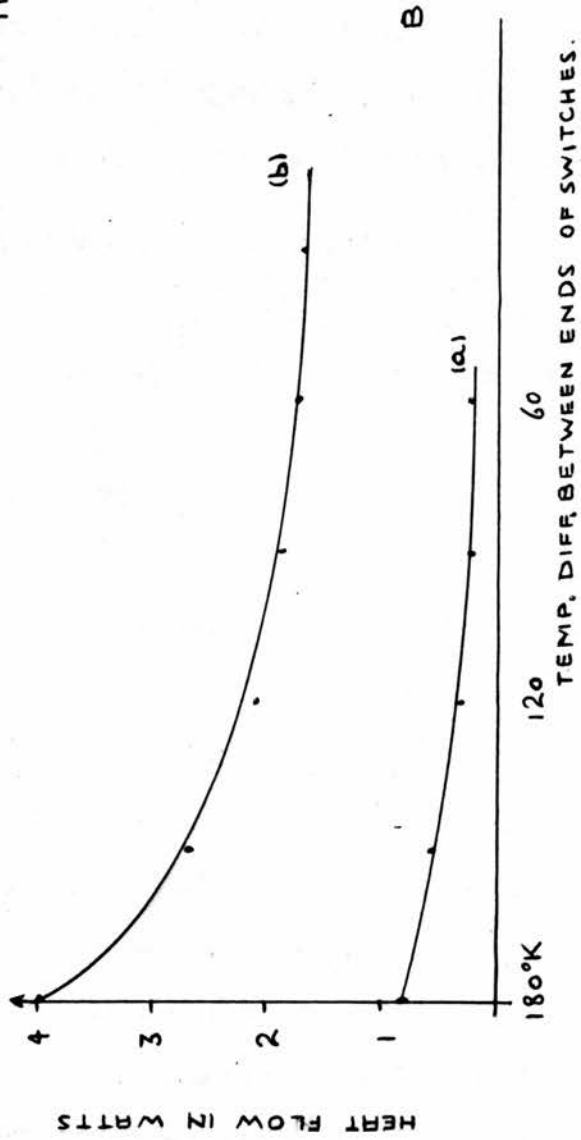
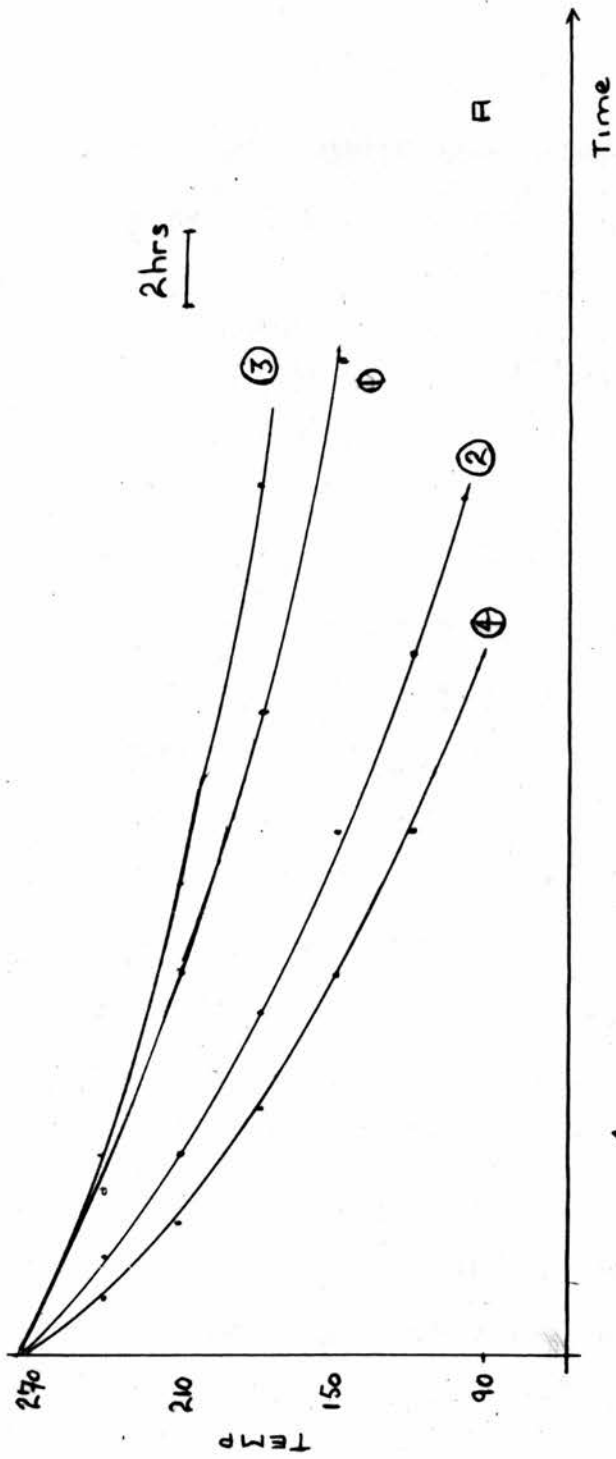


Fig. No. 9.
Cooling Curves.

of the jig.

The efficiency of the switches was further improved by coating all contact interfaces (spade terminals etc.) with a thin layer of indium (~ 0.5 mm.).

(c) Efficiency and Performance

Shown in Fig.9.A are four cooling curves, obtained under different conditions of operation of the heat switches. Curve 1 was obtained in the manner originally intended for the first cooling stage from room temperature to approximately 120°K. This was done by filling the nitrogen can and closing both switches. The conduction path, however, proved too long (~ 22 ins.) and the resultant cooling time was of the order of 30 hours. In order to decrease this cooling time, it was decided to allow a small amount of liquid nitrogen (~ 150 c.c.) into the hydrogen can and use only the lower switch for the primary cooling. 2 is the cooling curve obtained in this way, showing that a decrease of about 50% is achieved in cooling time. As a comparison, curve 3 gives the conduction and radiation losses to the dilatometer working under the same conditions as 2 with the switch open.

The fourth curve shows the cooling rate which can be achieved by closing the diffusion pump and allowing some helium exchange gas into the outer can. Although this

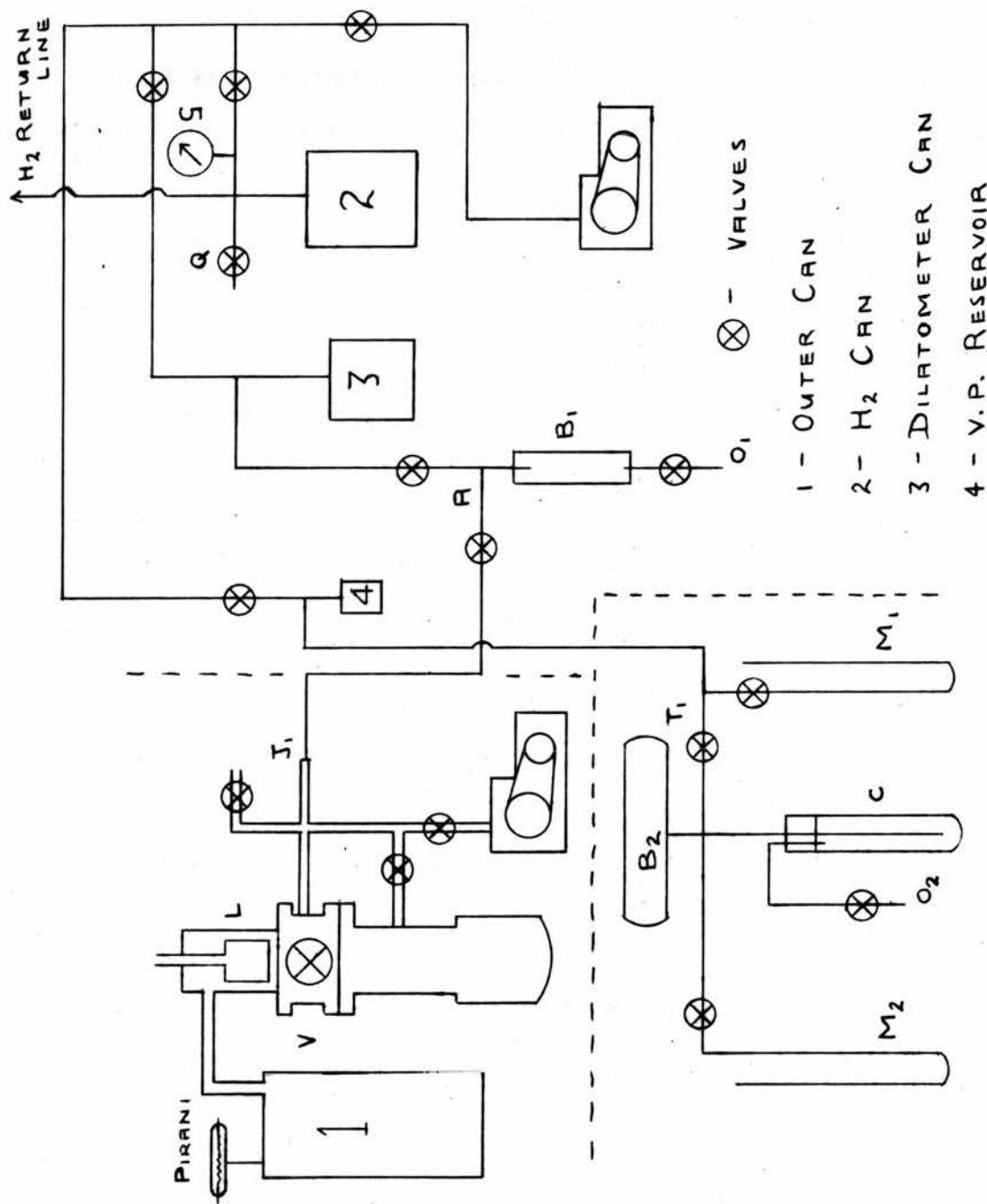


Fig. No. 10.
The Pumping System.

gives the fastest cooling rate, it is not profitable from the point of view of loss of liquid nitrogen due to convection heating from the outer can. The graphs show, however, that the mechanical heat switch gives a comparable cooling rate to what must be the most effective helium gas switch.

The curves of Fig.9.B giving heat flow versus temperature difference, between the ends of the switches, show that although the heat flow is quite large, the mass of the dilatometer and can (~ 2450 gms.) is such that the cooling time is necessarily long. Curves a and b correspond to curves 1 and 2 of the other graph.

The results shown in the two graphs are based on rough readings taken during actual experiments with the whole apparatus and are given only as an indication of the efficiency. Time did not permit close inspection to find the effect of increasing the force on the levers.

II.IV.5 Pumping System

A schematic diagram of the pumping system is given in Fig.10. The double lines indicate metal tubing (for the most part 1/2 in. diameter copper) and the single lines indicate glass tubing. The dotted dividing lines show that the system breaks down into three parts.

The outer can (1) is continuously pumped to maintain

a vacuum of about 10^{-6} mm. Hg, with an Edwards 'Speedivac' oil diffusion pump (Model 203) backed by an Edwards rotary pump (Model 1 SC 50 B). The diffusion pump is surmounted by a baffle valve V and a liquid air trap L, which is connected to the can via a short length (~ 12 ins.) of 1 in. diameter copper tubing. The length of glass tubing J,A was incorporated so that it might be possible to allow a few mm. of helium gas into the outer can, should this prove necessary or convenient at any time. Four Saunders 1/2 in. valves are used in this part of the pumping system.

One Edwards rotary pump (Model 2 SC 20 A) is used for the rest of the pumping system, but each part can be pumped separately. Two connections are made to the tube from the dilatometer can (3), one straight to the pump and the other to a glass bulb B, which is open ended at O_1 . When operating the apparatus, a few centimetres of helium gas (the pressure is indicated on a small manometer fixed to B_1) is let into the bulb at O_1 and this can then be used as exchange gas in the dilatometer or the outer can. The outlet tube from the hydrogen can has one connection to the pump, one to the hydrogen return line leading to the storage vessels and a third through a quick release valve Q to the open air. A 30-0-30 Eudenberg gauge G is mounted near the can.

The pumping system associated with the vapour pressure thermometer consists of two mercury manometers M_1 , M_2 , a glass bulb B_2 of capacity three litres, and a charcoal trap C. The purpose of these is given in section II.VI.6 when discussing the calibration of the platinum resistance thermometer.

II.IV.6 Temperature Measurement and Control

A platinum resistance thermometer is used for the temperature measurement as, with suitable calibration, it can be used over the whole range and also has the advantage of being extremely sensitive to small temperature drifts. The thermometer is wound from 47 s.w.g. 'Thermopure' wire which was annealed before winding by electrical heating. The wire was wound on cigarette paper shellaced to a copper former. The ends were tied with cotton and a second coat of shellac applied to hold the turns in place. The former was then slid into position inside the dilatometer case (Fig.2) and the ends of the wire soldered to the bus bars.

(a) Measurement

A potentiometer method is used for measuring the resistance. As lack of space made it necessary to place the temperature measurement system a fair distance from

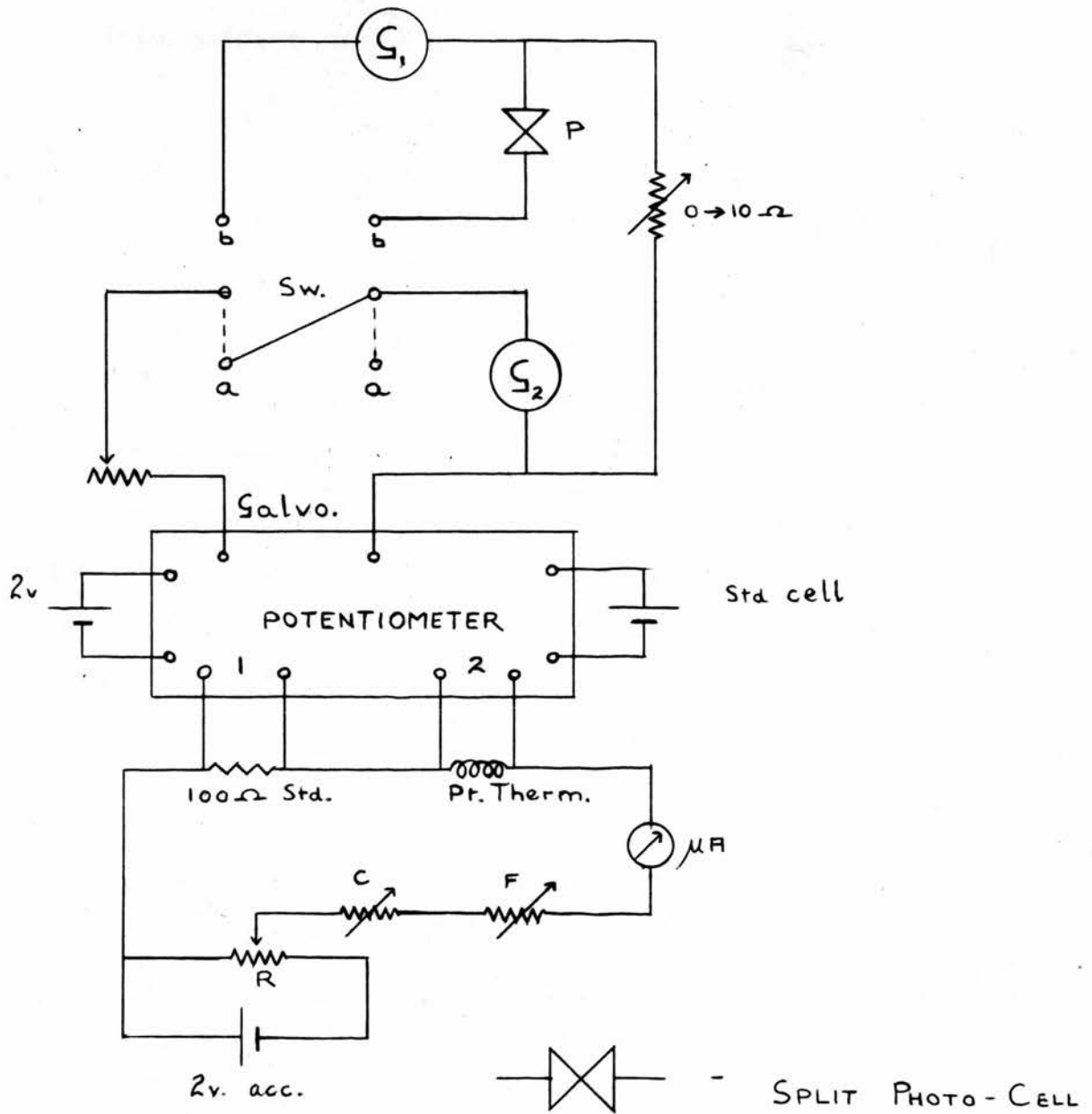


Fig. No. 11.
Temperature Measurement System.

the cryostat, the potentiometer has the advantage over a Wheatstones bridge, in that there is no problem with the long leads required.

The instrument is a direct reading potentiometer (H. Tinsley and Co.Ltd. - Type 4025) which is used in the circuit shown in Fig.11. The current through the thermometer, drawn from a 2 volt accumulator, is controlled by the rheostat R and the coarse and fine controls, C, F. A micro-ammeter, μA , is included to give a rough indication of the current draw. When taking a resistance reading, the current is altered until the voltage across the 100 ohm standard resistance is exactly 20 milli-volts. The voltage across the thermometer is then equal to twice the resistance. This method gives a direct reading of resistance and makes temperature control much easier.

The galvanometer amplifier arrangement described by MacDonald²⁸ is used as detector of balance. This arrangement using two simple robust galvanometers G_1 , G_2 and a split photo-cell P, couples a high degree of sensitivity with a very high input impedance and a stability against vibration, making it much more suitable than a single sensitive galvanometer. The switch SW, in position a, isolates the secondary galvanometer G_2 to get a rough indication of voltages before bringing the primary

galvanometer G_1 and photo-cell (housed in a separate box) into the circuit.

(b) Sensitivity

The accuracy required of the temperature measurement is governed by the sensitivity of the dilatation measurements, in that a change of temperature corresponding to the minimum detectable dilatation must be readily observed. In this case, assuming a dilatation of 0.5×10^{-7} and differential expansion coefficient of 10^{-5} , the corresponding temperature change is $.006^{\circ}\text{K}$.

The thermometer has an ice point resistance of 87.633 ohms and a resistance/temperature gradient of approximately 0.36 ohms/degree. Thus a temperature change of .006 degrees is equivalent to a resistance change of approximately .002 ohms, implying that the resistance must be measured to three places of decimals. The arrangement can be made sensitive enough to detect a resistance change of 5×10^{-5} ohms, but in practice it was not found possible to hold the temperature steady to better than 10^{-3} of a degree over a long period of time (~ 2 hours). The additional sensitivity, however, proves extremely useful when controlling the temperature, as it is possible to detect and compensate for very small regular temperature drifts.

(c) Calibration

As the dilatometer is never in direct contact with the coolant liquids, the vapour pressure thermometer had to be incorporated on the lower deck to calibrate the platinum thermometer. The vapour pressure thermometer, moreover, has the advantage that many more calibration points can be obtained than if only the boiling points of the coolant liquids are used.

Calibration points were taken when the dilatometer was being pre-cooled for an experimental run. The reservoir and measuring system (Fig.10) are pumped for about 24 hours before using to expel water vapour etc. The gas to be used for the calibration is then allowed into the system at O_2 and the bulb B_2 is filled to a pressure slightly above atmospheric with tap T_1 closed. The dilatometer is cooled to a temperature lower than the boiling point of the gas and the temperature is held steady with the electrical heater. Some of the gas is condensed into the reservoir by opening tap T_1 for a reasonable time (~ 30 mins.). Another hour is required to reach an equilibrium state and the vapour pressure is read from manometer M_1 using a cathetometer. Further calibration points, using the same gas, are obtained by simply cooling the system as it stands to another equilibrium state.

Vapour pressure tables are used for the final stage of the calibration. This method gives extremely accurate calibration points because of the very high temperature dependence of the vapour pressure. The ice-point, taken as 273.15°K was found by surrounding the dilatometer can with pure ice which was continuously stirred till the resistance became constant.

(d) Temperature Control

The dilatometer can is at all times subject to a cooling effect due to radiation from the nitrogen can and conduction from the hydrogen can. To attain temperature equilibrium of the dilatometer, this cold leak is balanced with an electrical heater wound on the outside of the dilatometer can. This heater consists of 100 turns of 30 s.w.g. constantan wire, shellaced into place and giving a resistance of approximately 150 ohms. The heater input is fed from the mains through a 30 volt transformer and is controlled by a variable transformer and a fine control variable resistance in series with the heater.

To attain any desired temperature, the dilatometer is cooled by closing the lower heat switch. When a temperature a few degrees above that required is indicated, the heat switch is opened and the heater is switched on to balance out the cold leak. Because of the relative remoteness

of the heater with respect to the dilatometer, a period of about 1/2 an hour is required to attain a constant reading on the potentiometer. To speed up the attainment of equilibrium, the dilatometer can be filled with helium exchange gas to a pressure of a few centimetres of mercury. The dilatometer is cooled further, as before, and another equilibrium stage attained with a lower heating current.

As the heater voltage is subject to fluctuations of mains voltage, an improvement in control stability could probably be achieved by using a stabilised D.C. heater supply.

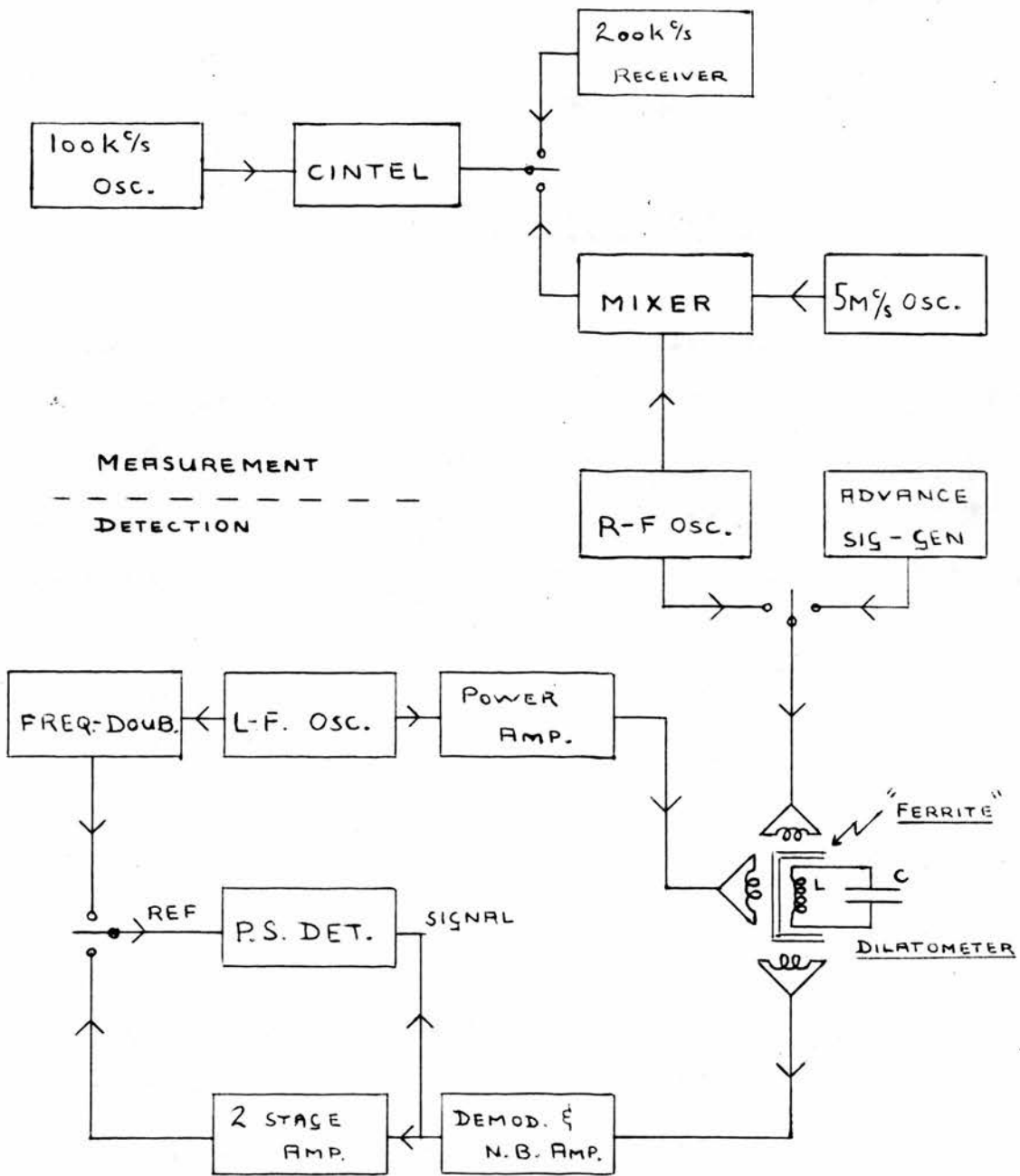


Fig. No. 12.
Block diagram of Electronics.

CHAPTER III

APPARATUS II (ELECTRONICS)

At each temperature equilibrium stage of the dilatometer, the electronic measurements consist of (a) a detection of resonance in the L.C. tank circuit and (b) a count of the resonant frequency. The two electronic systems are almost completely independent, having as a common unit the R.F. oscillator. The present set up, shown in the block diagram of Fig.12 is a development of ^{the} original system described in this chapter. Chapter IV deals with the modifications which proved necessary as the apparatus was improved.

III.I Operating Frequency

To determine the optimum values of working frequency and frequency range of the R.F. oscillator, the available frequency measuring equipment had to be considered. This was a 'Cintel' automatic frequency monitor (1 Mc/s). Thus the maximum permitted resonant frequency change $\Delta \nu_0$ (equation 4) in the tank circuit, over the temperature range considered, is 1 Mc/s.

The second condition governing the operating frequency is that of maximum possible sensitivity. Assuming a gap length x of the dilatometer condenser, with a specimen of length l and coefficient of expansion α , the relative resonant frequency change caused by a temperature change T is given by

$$\frac{dv}{v}_0 = \frac{1}{2} \frac{\delta l}{x} = \frac{1}{2} \frac{\delta l}{l} \frac{l}{x} = \frac{1}{2} \alpha T \frac{l}{x} \quad (5)$$

Substituting relevant values for α and $\frac{l}{x}$ with T taken as 250°K gives

$$\frac{dv}{v}_0 = \frac{1}{5}$$

The sensitivity considerations of section (II.II.3) show that for any temperature interval considered, greater sensitivity is achieved the greater is dv_0 . As the maximum possible value of dv_0 is 1 Mc/s, the operating frequency must be of the order of 5 Mc/s.

III.II Frequency measurement

The frequency count is obtained by mixing the signal from the R.F. oscillator with that from a standard 5 Mc/s source and counting the resultant difference frequency on the Cintel. Gate control pulses in the counter are produced from an external 100 k c/s reference source and it was intended to use this 100 k c/s reference as a signal

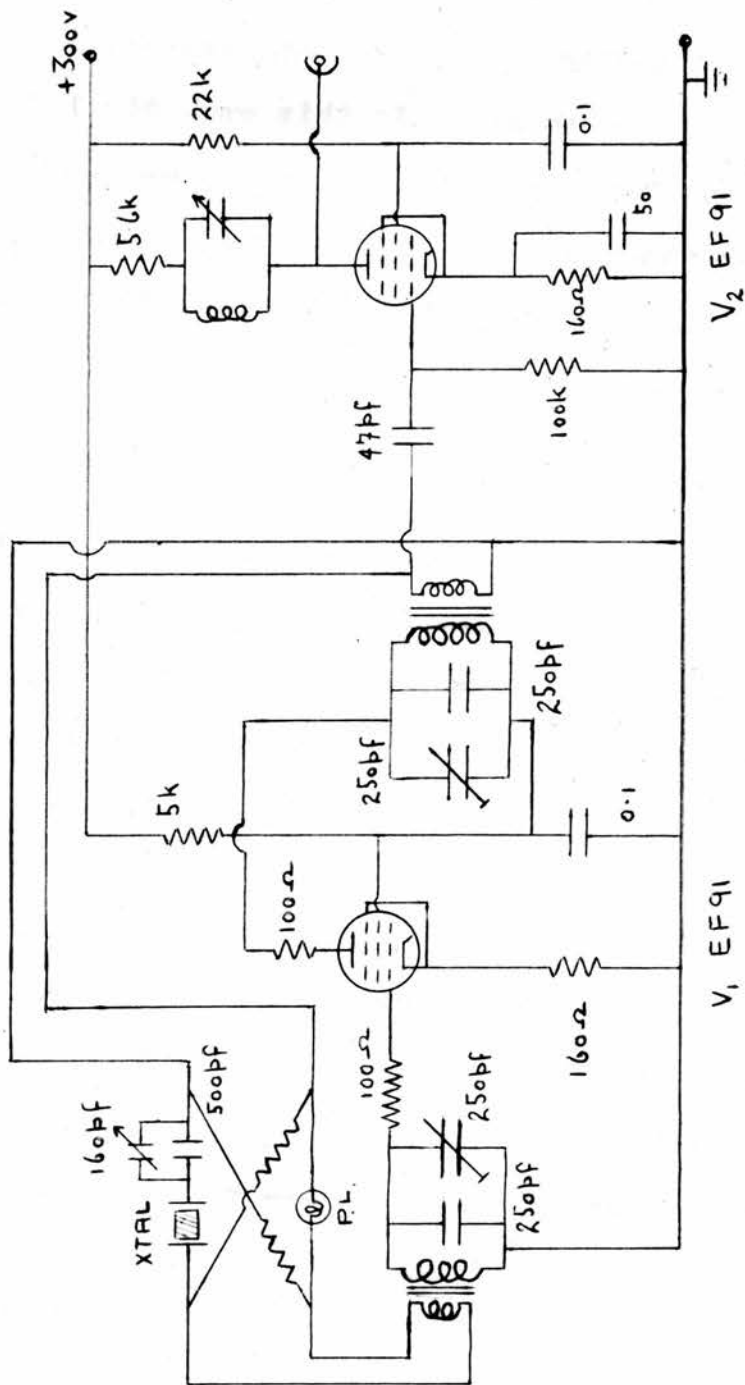
from which to derive the 5 Mc/s standard.

III.II.1 R.F. Oscillator

The R.F. oscillator was designed to operate in the range 5-6 Mc/s. The circuit shown in Fig.13 employs three EF91's. The first two, comprising the oscillator (which is a push-pull development of the Clapp oscillator²⁹) are a matched pair as regards (gm - eg) and the third is a buffer stage acting as an A.G.C. amplifier. Initially, the buffer stage incorporated a low Q, tunable, anode load, but it was found that this stage tended to lead the oscillator and to cause undesired effects in the detection system, which could not be completely understood, but which disappeared with the insertion of the resistive load.

The tank circuit consists of a high Q (≈ 200) coil wound on a ceramic former for maximum stability³⁰ and the condenser arrangement shown in the diagram. C₁ and C₂ are good quality ganged condensers which are tuned with slow motion drives. A simple mathematical analysis shows that it is possible, with this arrangement, to alter the frequency of the oscillator to within 1 c/s of any desired value.

The circuit was built into two very substantial brass boxes for shielding and thermal stability. The L.C.



 P.L. - PILOT LIGHT
 60V, 0.04A

Fig. No. 14.
100 kc/s Oscillator.

frequency determining circuit is in one and the remainder of the electronics in the other. In this way, the L.C. circuit is protected from the effect of component heating which occurs in the other box. Further thermal shielding is afforded by lining the interior of the box with 'jabolite' (extended polystyrene).

III.II.2 100 kc/s Oscillator

The circuit of Fig.14 is the 100 kc/s oscillator which was built to monitor the cintel. The circuit is of the Meacham Bridge type³¹ using a quartz crystal operating in a thermostatically controlled oven. The short term stability of this crystal as quoted by the manufacturers (Salford Electrical Instruments Ltd.) is of the order of 5 parts in 10^6 or better. As the overall measuring accuracy of the counter is that of the reference source \pm a small correction, it was essential to get a very accurate check on both the long term and short term stabilities of the oscillator. The simplest way to do this was to feed a signal of known frequency to the counter and find the divergence of the count, thus giving directly the error in the 100 kc/s reference signal.

Since no suitable standard existed in the lab, it was decided to make use of the B.B.C. 200 kc/s Droitwich

signal which is known to have a frequency stability of the order of 1 part in 10^8 . The simple receiver shown in Fig.15.a was built to feed the counter, but it was found that the A.F. modulation of the carrier made it impossible to take an accurate set of readings. Since at no time during the day is the carrier wave transmitted without modulation for a reasonable time, it proved necessary to add the Schmitt trigger circuit (Fig.15.b) onto the receiver. This gives a roughly square shaped wave of amplitude independent of the percentage modulation, unless this modulation approaches 100%.

A check on the readings taken over a period of several weeks showed that although the short term stability was at least 2 parts in 10^6 , there was a day to day drift of the oscillator frequency of the same order of magnitude and that this drift followed no regular pattern as regards rise and fall.

Because of the uncertainty of the long term stability of the above oscillator, it was decided to buy a commercially built 100 kc/s oscillator, (Bradley and Co.Ltd. - Type UE.6) which is specified to have a long term stability of the order of 1 in 10^7 . A similar check to that described above was undertaken and the results showed that the stability is probably slightly better than specified.

It was observed that when a set of frequency readings, taken at equal time intervals with the original oscillator as monitor, were plotted against the time, the resultant curve in every case was approximately sinusoidal. The peaks and troughs of these curves were then found to coincide with the 'on-off' periods of the heater controlling the temperature of the oven in the crystal holder. This recurring, regular, periodicity would seem to indicate the strong resonant frequency/temperature dependence of the quartz crystal³². Further, if more stringent precautions were taken to ensure greater temperature stability the short term frequency stability of the oscillator would probably be greatly improved.

III.II.3 5 Mc/s Standard

The 5 Mc/s oscillator is a quartz crystal oscillator by Standard Telephones and Cables Ltd. (Type 90/LQE/811). The stability is assumed to be at least equal to that specified, i.e. ± 4 parts in 10^9 , as there is no equipment available to make a conclusive check. Any breakdown, however, would be observed as instabilities in the frequency counts of the R.F. oscillator. The power supply required for this unit is described in section III.III.3.

As mentioned previously, it was intended to derive

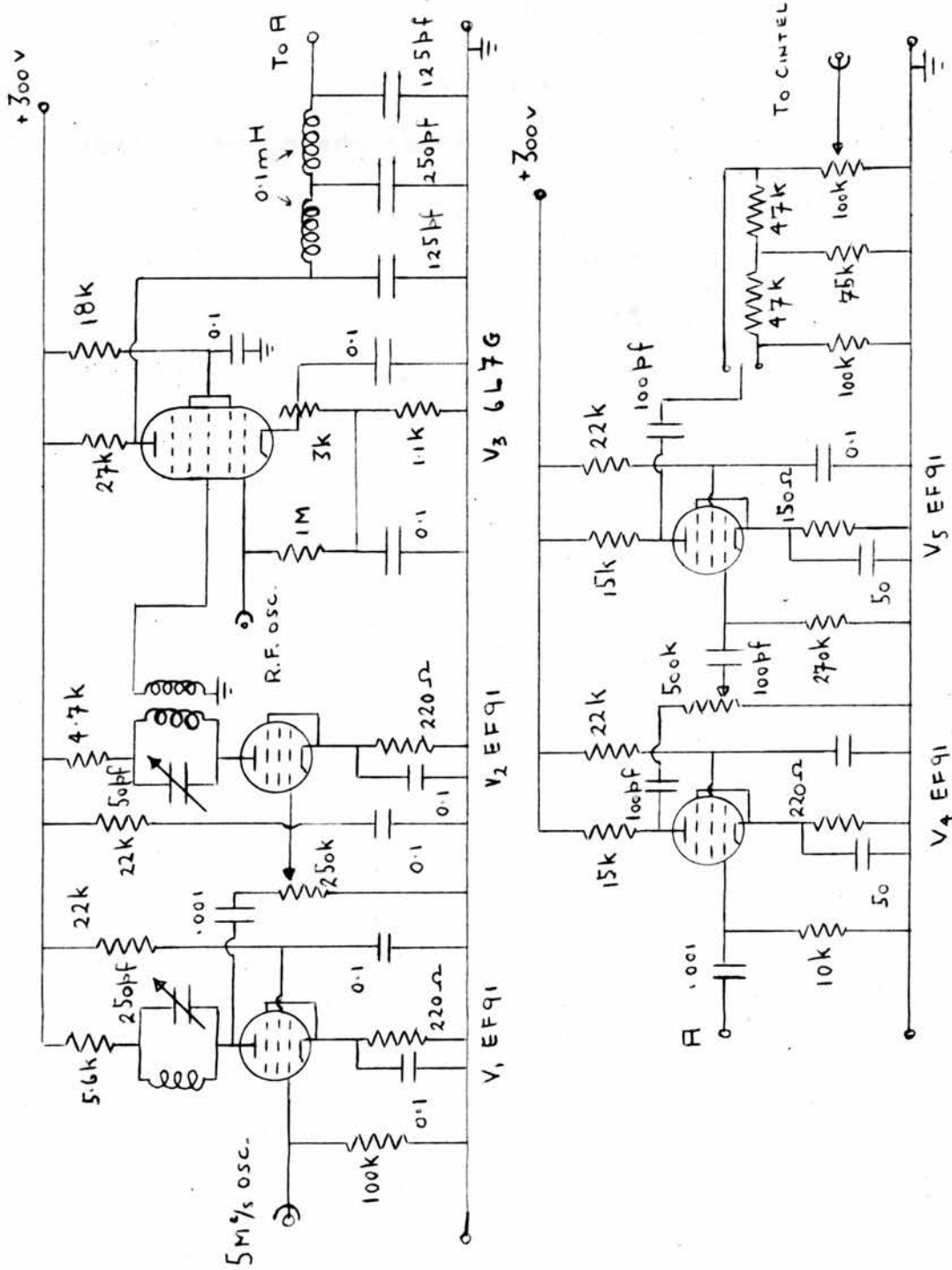


Fig. No. 16.
The Mixer.

the 5 Mc/s standard from the 100 kc/s oscillator. This would have involved a multivibrator chain and a series of crystal filters. An attempt was made to build such a circuit before it was known that a 5 Mc/s oscillator could be bought. Only L.C. filters were used, however, and the circuitry proved too complicated.

III.II.4 The Mixer

The mixer circuit (Fig.16) is straight forward, employing a 6L7G pentagrid mixer valve, V_3 . The output of the 5 Mc/s oscillator is fed to grid g_3 through the amplifying stages V_1 , V_2 giving a gain of about 100. Low Q tuned anodes are used to ensure that there is no tendency to lead the oscillator. Amplifying valves V_4 , V_5 and the low pass filter ensure that the difference frequency output is free from high frequency components. The switched attenuator in the output is to keep the output voltage within the limits required for the counter (0.2 - 2 volts r.m.s.).

III.II.5 Performance

Tests on the stability of the R.F. oscillator, using the above system, showed that the frequency drifts at a rate varying from 1 cycle/minute to 4 cycles/minute. Readings,

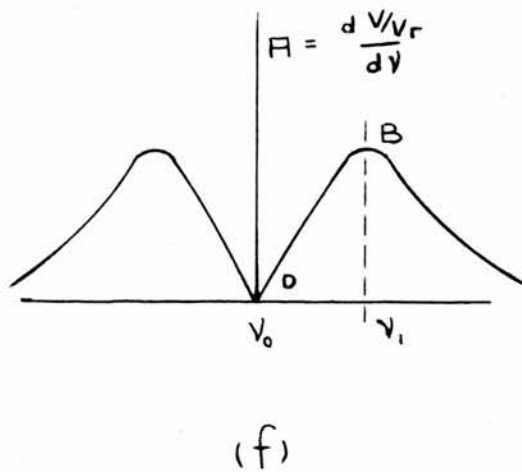
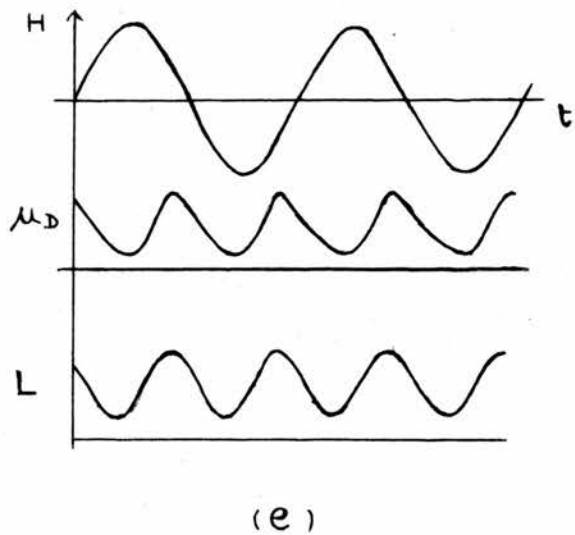
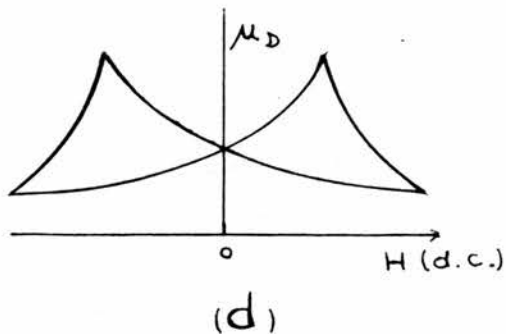
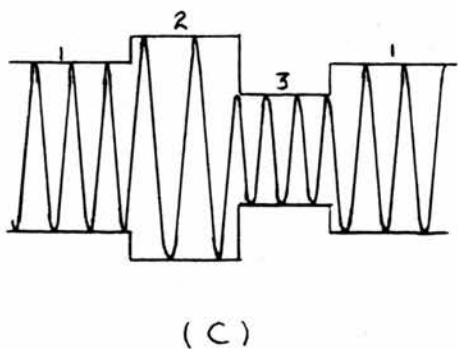
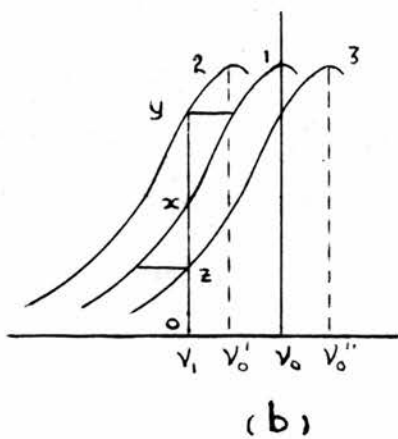
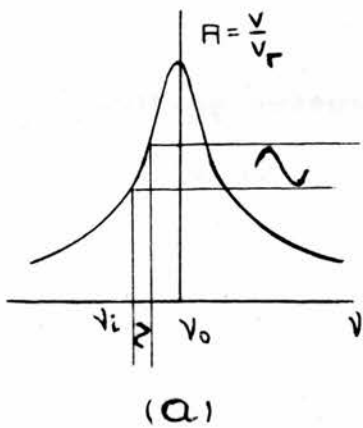


Fig. No. 17.
Principle of the Method.

however, taken every 10 seconds for extended periods showed that the drifts are regular, i.e. consecutive readings show the same tendency. For a period of time, therefore, long enough to make the necessary measurements (an estimate of 15 seconds is very generous) the maximum error in frequency count is less than 1 part in 5×10^6 .

III.III Resonance Detection System

Before giving a description of the electronic units associated with the detection system, it is necessary to indicate the principles underlying the method used in order to show more clearly the purpose of each unit.

III.III.1 Principle of the Detection

When a variable R.F. signal is applied to an L.C. resonant circuit, the voltage in the circuit, which can be obtained from a coil loosely coupled to the inductance, has the frequency dependent characteristics given by a simple resonance curve (Fig.17.a). Resonance occurs at the value of frequency ν_0 given by the relation

$$\nu_0^2 = \frac{1}{4\pi^2 LC} .$$

If the input frequency ν_1 is frequency modulated the output R.F. carrier from the pick-up coil is amplitude modulated at the sweep frequency, and if the amplitude of

the sweep is very much smaller than the line width of the resonance curve, the modulation amplitude is equal to the derivative of the resonance curve. Fig.17.f shows the modulus of the derivative, the two peaks corresponding to the inversion points.

The resonant frequency ν_0 can, in theory, then be found by phase sensitive detection using the derivative or by linear detection using the modulus of the derivative, after demodulation of the R.F. carrier. The practical difficulties of this method are in measuring the carrier frequency after detecting resonance and designing an oscillator of sufficient stability coupled with some means of sweeping the frequency.

The same effect, however, is achieved by "sweeping the resonance curve". Suppose as in Fig.17.b the resonant frequency of the L.C. circuit can be caused to change either magnetically or electrostatically to any one of the values ν_0 , ν_0' , ν_0'' . For an input frequency ν_1 , the amplitude of the pick-up signal can be changed from ox to oy to oz by changing the resonant frequency of the circuit. (Fig.17.c shows the output amplitude in terms of the three conditions of the system.) If now the resonant frequency is swept periodically between these limits, the output R.F. carrier from the pick-up coil will be amplitude modulated at the

sweep frequency, and the same considerations for detection as above will hold.

The mechanism for sweeping the resonance curve must be inherent in the tank circuit, and since there are only two components, there are basically only two methods possible. The most obvious, would appear to make use of some form of vibrating reed condenser, but it was felt that mechanical vibrations inside the cryostat might give rise to mechanical resonances. The desired effect, however, can be obtained by using a ferrite as the core of the inductance.

When a ferromagnetic material is subject to a polarising, unidirectional, magnetic field, upon which is superimposed an alternating magnetic field, the resultant permeability is known as the incremental or reversible permeability and is defined as

$$\mu_D = \Delta B / \Delta H.$$

The value of μ_D is shown as a function of D.C. magnetic field strength in Fig.17.d. This curve is known as a "butterfly curve".

The assumption drawn from the butterfly curve was that if a low frequency sinusoidal magnetic field H is applied to such a core, the incremental permeability should vary approximately sinusoidally between the limits given by the

curve. As a first approximation, the inductance of a coil with such a ferrite core can be taken as proportional to the permeability, i.e. $L = k\mu_D$, implying that the inductance of the coil should also vary sinusoidally between some upper and lower limits as shown in Fig.17.e.

In order to test the assumption, a rough experimental set up was built using a circular ferrite core for the inductance. The low frequency sweep was taken straight from a variac and the output from the pick-up coil displayed on a C.R.O. This very rough check proved satisfactory, in that as the R.F. carrier signal was swept through resonance, the amplitude modulation on the pick-up signal disappeared. This was necessarily only a qualitative result, but it was decided to continue with this approach.

It must, however, be noted that the frequency of the amplitude modulation is twice that of the low frequency sweep. (Fig.17.e.)

III.III.2 Electronic Units

Phase sensitive detection is employed for maximum sensitivity. The detector signal is derived from the R.F. carrier by the demodulator and narrow band amplifier, and the detector reference is taken from the low frequency oscillator.

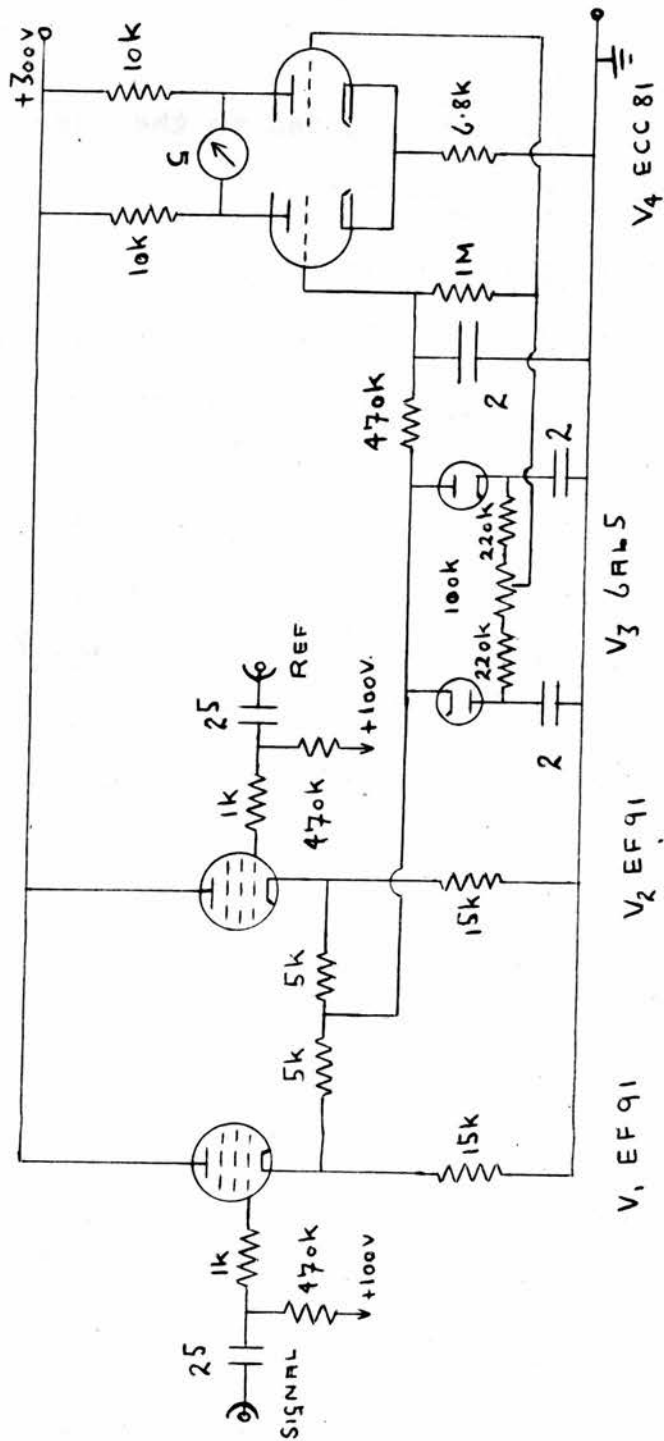


Fig. No. 20.
P.S. Detector I.

(a) Low Frequency (L.F.) Oscillator and Power Amplifier

The oscillator is of the Wien bridge variable frequency type³⁴ operating at 160 c/s and is formed by the first three stages of Fig.18. Automatic amplitude control is incorporated in the circuit by using a thermistor, (Standard Telephones and Cables - A/5513) with a negative coefficient of resistance as the limiting element. Highly stable components are used in the frequency determining bridge network (R.C.) for maximum frequency stability. Two outputs are taken from the oscillator, $O_1 \sim 30$ volts r.m.s to the reference input of the phase sensitive detector and O_2 to the phase splitter valve V_4 .

The power amplifier is a normal push-pull amplifier operating under class-A conditions, delivering approximately 5 watts to the load. Two beam tetrodes (V_5, V_6) are fed from the phase splitter valve. The amplifier is matched to the sweep coil, which has a resistance of approximately 4 ohms, by a 10:1 ratio audio transformer.

(b) Demodulator and Narrow Band (N.B.) Amplifier I

The demodulator (Fig.19) is a simple diode detection circuit using a germanium diode V_2 . The narrow band amplifier V_4, V_5 employs a tunable twin-T feedback network³⁵ in preference to an L-C tuned circuit. The gain of this amplifier is of the order of 400 with a bandwidth of

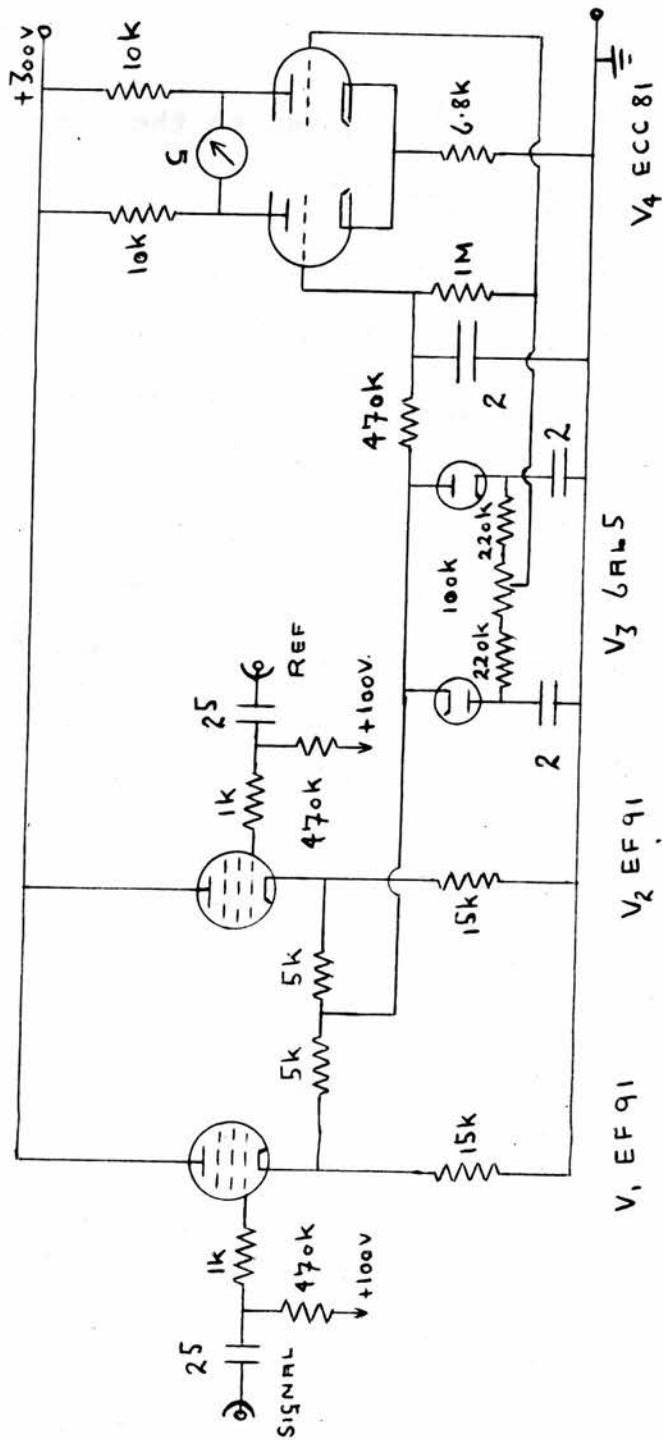


Fig. No. 20.
P.S. Detector I.

approximately 10 c/s. The output of this circuit (~ 50 volts at the inversion peaks) is fed to the phase sensitive detector through the phase shifting valve V_6 .

(c) Phase Sensitive (P.S.) Detector I

Because of the frequency discrepancy noted in section III.III.1 of this chapter, a conventional P.S. detector could not be used. A similar situation arises, however, in measurements of second sound in liquid helium, i.e. when A.C. heating is applied to a wire in the helium, heat pulses in the liquid are produced at a frequency equal to twice the frequency of the A.C. heating current. The circuit shown in Fig.20 is one developed for use in second sound experiments, which has been adapted for the present work.

Signal and reference are mixed by the cathode follower valves V_1 , V_2 , and the resultant signal fed to the double diode bridge network V_3 . Correct phasing of the two signals causes a voltage across the grids of the difference amplifier V_4 .

III.III.3 Power Supplies

Three electronically stabilised power supplies were built, two at 300 volts and the other at 120 volts. The circuits of the two 300 volt supplies are similar, the

4 EL84'S IN PARALLEL

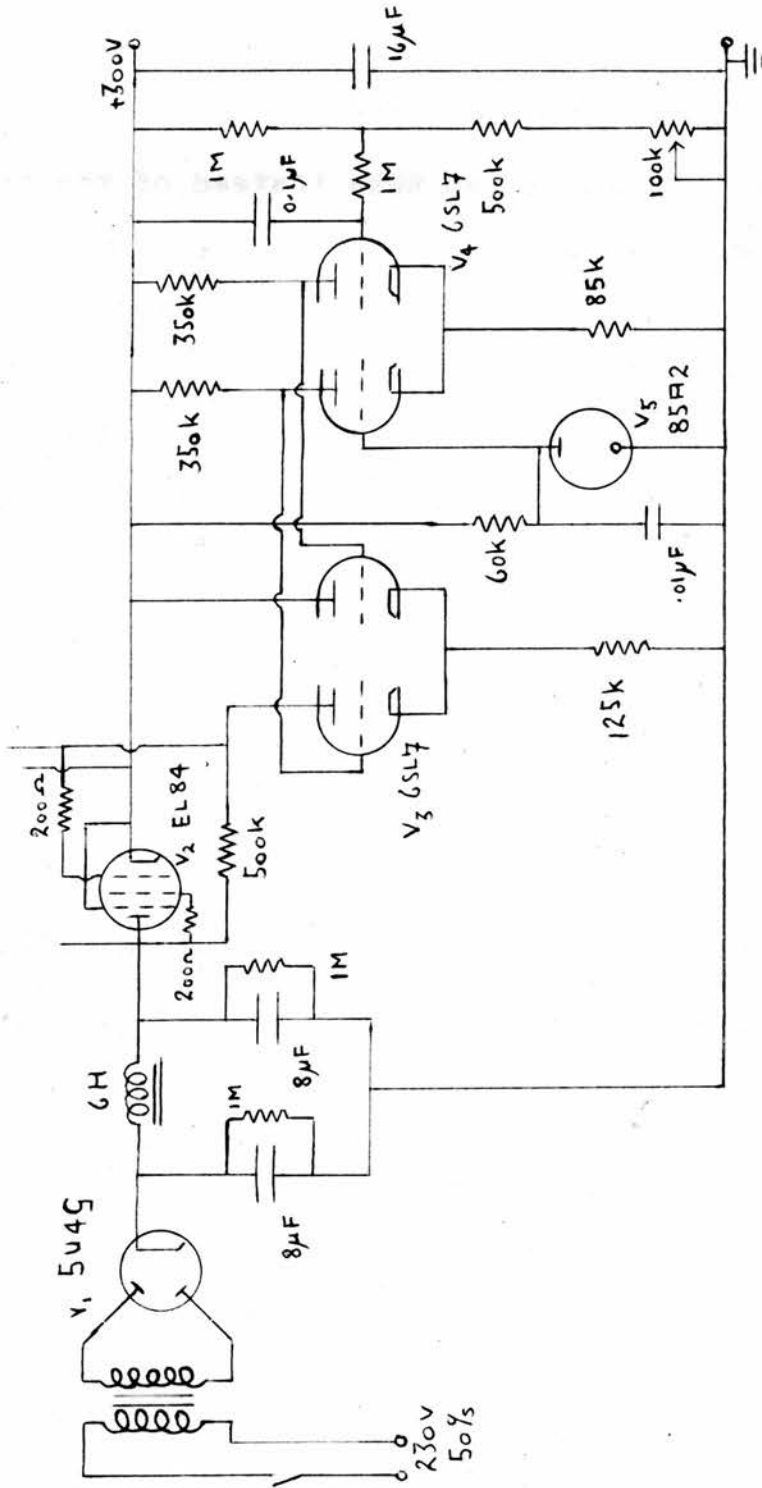


Fig. No. 21.
300 Volt Power Supply.

only difference being that in the second unit built, a 12E1 valve is used as the series tube instead of the bank of EL84's as shown in Fig.21. In both cases, the ripple content of the output is less than 5 millivolts peak to peak on load (~ 100 m.a.). The supply circuit for the 5 Mc/s oscillator (Fig.22) was built to confirm with the following required specifications:- 120 volts \pm 0.6 volts at 35 m.amps. The 50 c/s ripple from this supply is less than 1 m.volt peak to peak.

Two commercially built supplies (Solartron Electronics Ltd) are also used and the total power drain from all of the supplies is of the order of 140 watts.

III.III.4 Construction and Mounting of the Electronics

Each electronic unit is constructed on a separate panel and mounted vertically onto the 'Handy-Angle' framework (photo - Fig.23), so that the component wiring is facing forward. Each panel is actually a flat box with a shielding lid, held in position by self-tapping screws. This construction is extremely efficient, in that faults can be corrected with the unit in position and the shielding lid removed, whilst the complete units are readily demounted when necessary to make major circuit modifications.

The power supplies are constructed in a similar manner,

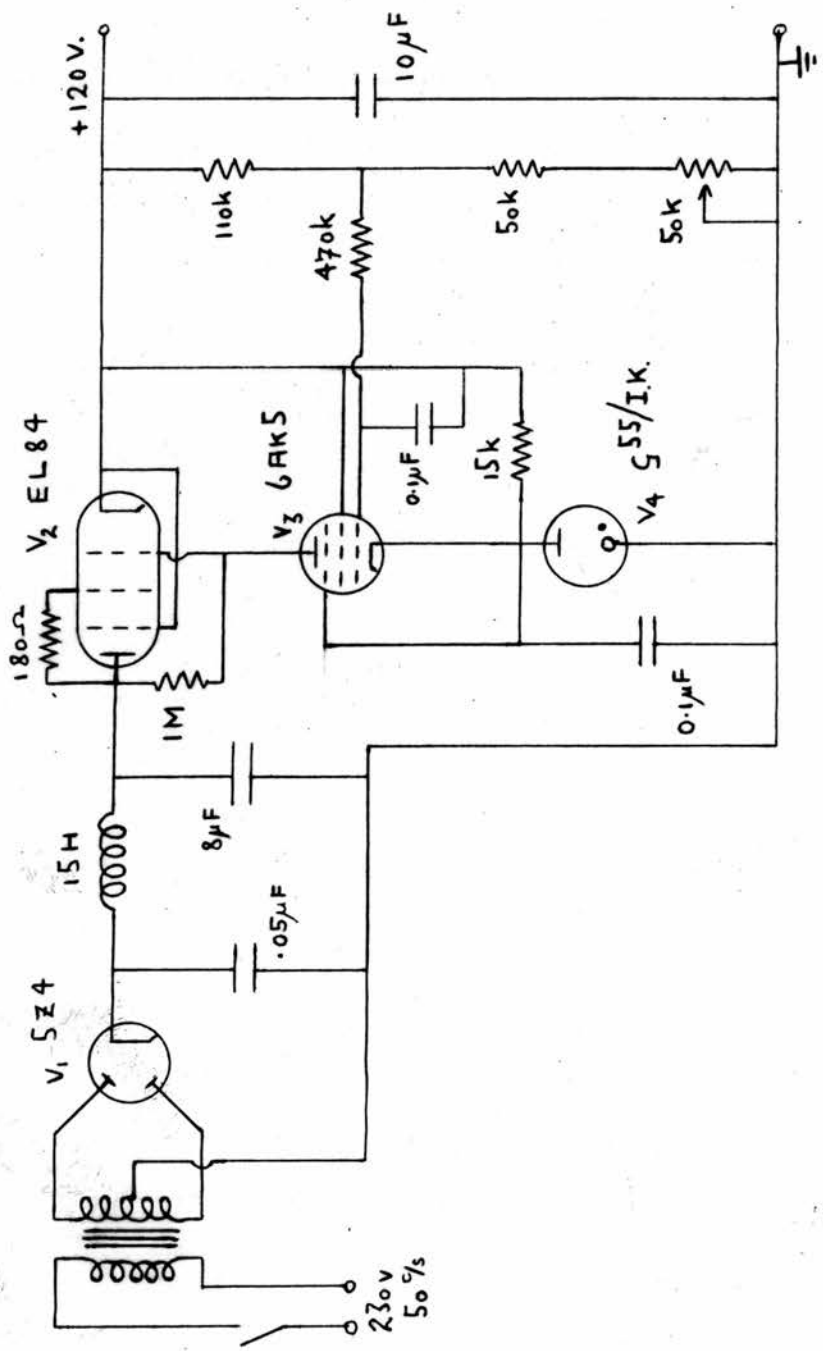


Fig. No. 22.
 120 Volt Power Supply.

but because of space limitation, these had to be mounted on a separate framework which is relatively inaccessible. Once constructed and mounted, however, the power supplies require little attention, and servicing poses few problems.

III.III.5 Ferrite Cores

Tests were made with various grades of ferrite to establish which would best satisfy the following requirements:-

1. Reasonable circuit Q (~ 10) at the operating frequency.
2. No significant reduction in Q value when cooled to the working temperature ($\sim 100^{\circ}\text{K}$).
3. Maximum amplitude modulation of the R.F. carrier for a given power input to the sweep coil.

The most suitable ferrite is a 'Gecalloy' product of Salford Electrical Instruments Ltd (Code No.CV54) giving a Q of slightly greater than 15.

The initial tests were carried out with circular cores, but these proved unsatisfactory in use. The most serious defect was the fundamental frequency coupling between the L.F. sweep coil and the pick-up coil. This pick-up resulted in a signal from the output of the N.B. amplifier at the frequency of the second harmonic. As this is the frequency of the modulation on the R.F. carrier, it caused a

non-reproducible zero error in the meter reading of the phase sensitive detector. In an attempt to eliminate this effect, it was decided to use an 'E-I' type transformer core in a manner similar to that used in the balanced saturable³⁶. The windings of the tank circuit inductance L, were equally divided on the outer limbs of the core and the sweep coil wound on the central limb. This gave a marked reduction in pick-up signal, but not sufficient to make this construction directly applicable.

The present construction makes use of the 'E-I' core, to supply the modulation, but the inductance is wound in two parts. Part is wound as above on the ferrite core and the remainder onto a perspex former. The pick-up coil is also wound on this former, and is thus isolated from the closed magnetic circuit of the ferrite. This gives a diminished R.F. signal, and also a reduced percentage modulation, but the output is free from L.F. pick-up. The photograph of Fig.27.a shows the inductance L as it is positioned on the top deck.

The sweep coil consists of 136 turns of 32 s.w.g. copper wire. When testing, several different sweep coils were used to find the optimum number of turns for matching to the power amplifier. This interchange of coils was

simplified by winding on square formers to fit the central limb of the core.



Fig. No. 23.

General View of Apparatus.

(Electronics rack and counting system
on the right, and temperature measure-
ment system on the left.)

CHAPTER IV

PERFORMANCE OF THE APPARATUS

IV.I Room temperature tests

Room temperature tests with the detection system of the previous chapter showed that the P.S. detector was inadequate both in sensitivity and balance stability. To remedy this failing, it was decided to build a conventional P.S. detector, and to derive the correct reference frequency from the L.F. oscillator through a frequency doubling circuit.

IV.I.1 The P.S. Detector II

The detector used is of the Schuster type³⁷. This circuit was chosen for its high balance stability and detector gain. The reference is fed to the cathode follower stage V_1 (Fig.24) which is transformer coupled in push-pull to the control grids of the gating valve V_3 of the cascode mixer. With no signal input, the output can be balanced with the 50 k pot.

The D.C. output, taken from the cathode follower V_4 is indicated on a 250-0-250 micro-ammeter, which is

protected against overloading by a series of switched resistors. For there to be no appreciable time lag between a change of frequency of the R.F. carrier and the subsequent change in meter reading, the output time constant R.C. is limited to a maximum of about 1 second. This is especially important in this set up, as the carrier frequency is swept manually.

IV.I.2 Frequency Doubler

The frequency doubler (Fig.25) comprises three valves. The first V_1 is an amplifier operating under class-C conditions with the anode load tuned to the second harmonic of the input signal³⁸. The following two stages V_2 and V_3 are tuned narrow band amplifiers preset with twin-T networks to the same frequency. The output (35 volts r.m.s.) is fed to the P.S. detector as reference. No provision is made for tuning this unit, so that it is necessary to "tune the signal" from the L.F. oscillator for maximum efficiency.

IV.I.3 Demodulator and N.B. amplifier II

The resultant increase in sensitivity achieved with the above modification showed up defects in the original N.B. amplifier (section III.III.2). Because of the very high magnification factor of the twin-T amplifying stage (V_3, V_4), it effectively filtered out of the noise in the

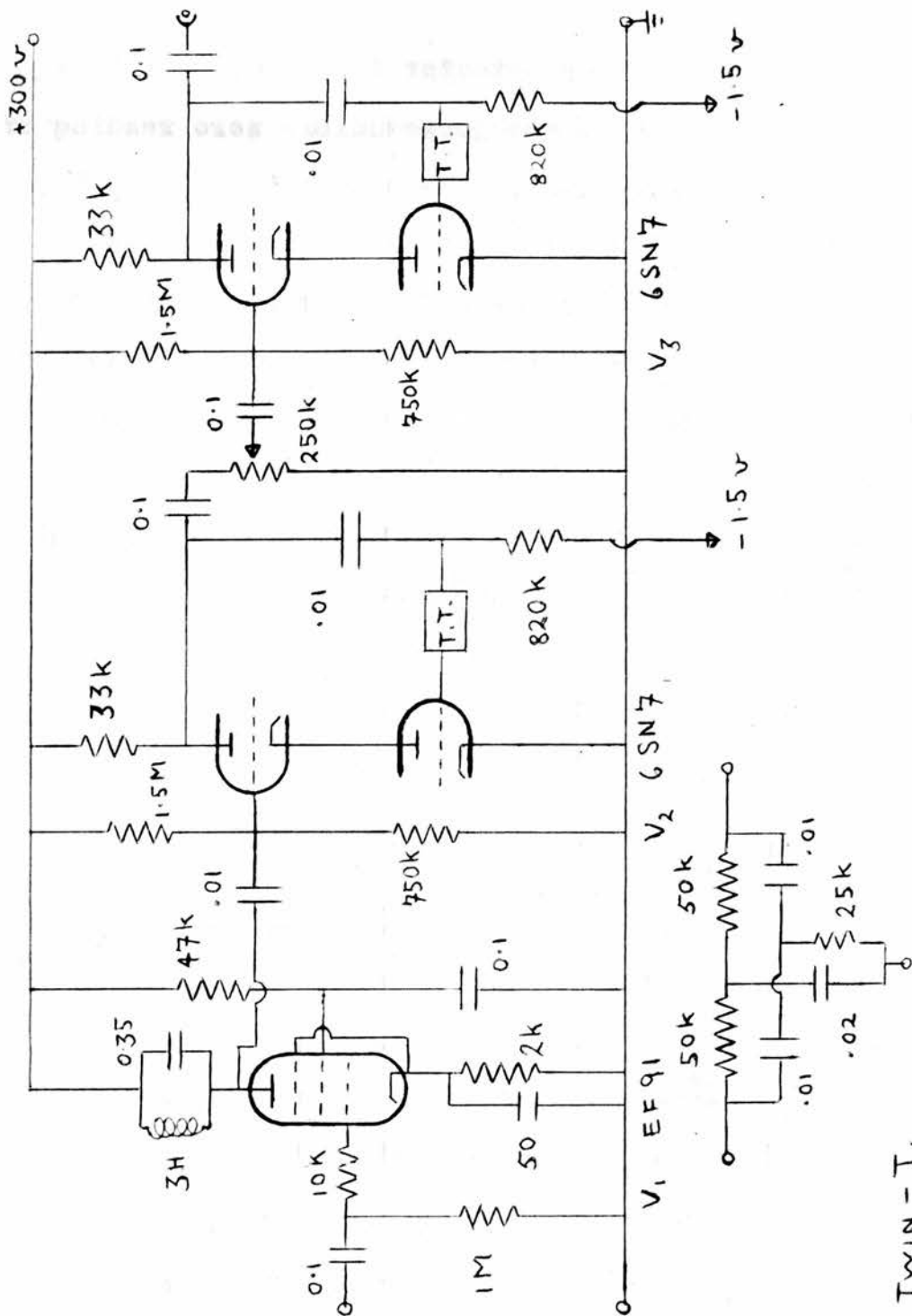


Fig. No. 25.
Frequency Doubler.

TWIN-T.

system a signal at the detector frequency. This coherent signal gave rise to a non-reproducible zero reading of the detector meter and made accurate detection impossible. Several combinations of demodulators and N.B. amplifiers were attempted to find the most suitable and although the circuit finally used (Fig.26) is extremely simple and straightforward, it was found to give the best results. The demodulator V_2 is a pentode biased to cut off for maximum gain. The main amplifying stage V_3 is a normal tuned anode load amplifier feeding into a cathode follower V_4 to eliminate oscillations in the amplifier. Two valves are employed in the phase shifter (V_5) to give a phase change of almost 180° .

IV.II Sensitivity

It has already been shown (section II.II.2) that the overall sensitivity of the apparatus is governed by the sensitivity of the resonant frequency detection. The following theoretical estimate, shows that the sensitivity required (i.e. detection of a dilatation of 0.5×10^{-7}) should be readily achieved with the present apparatus.

The voltage developed across the pick-up coil is of the form shown in Fig.17.a. For high Q, this curve is roughly given by

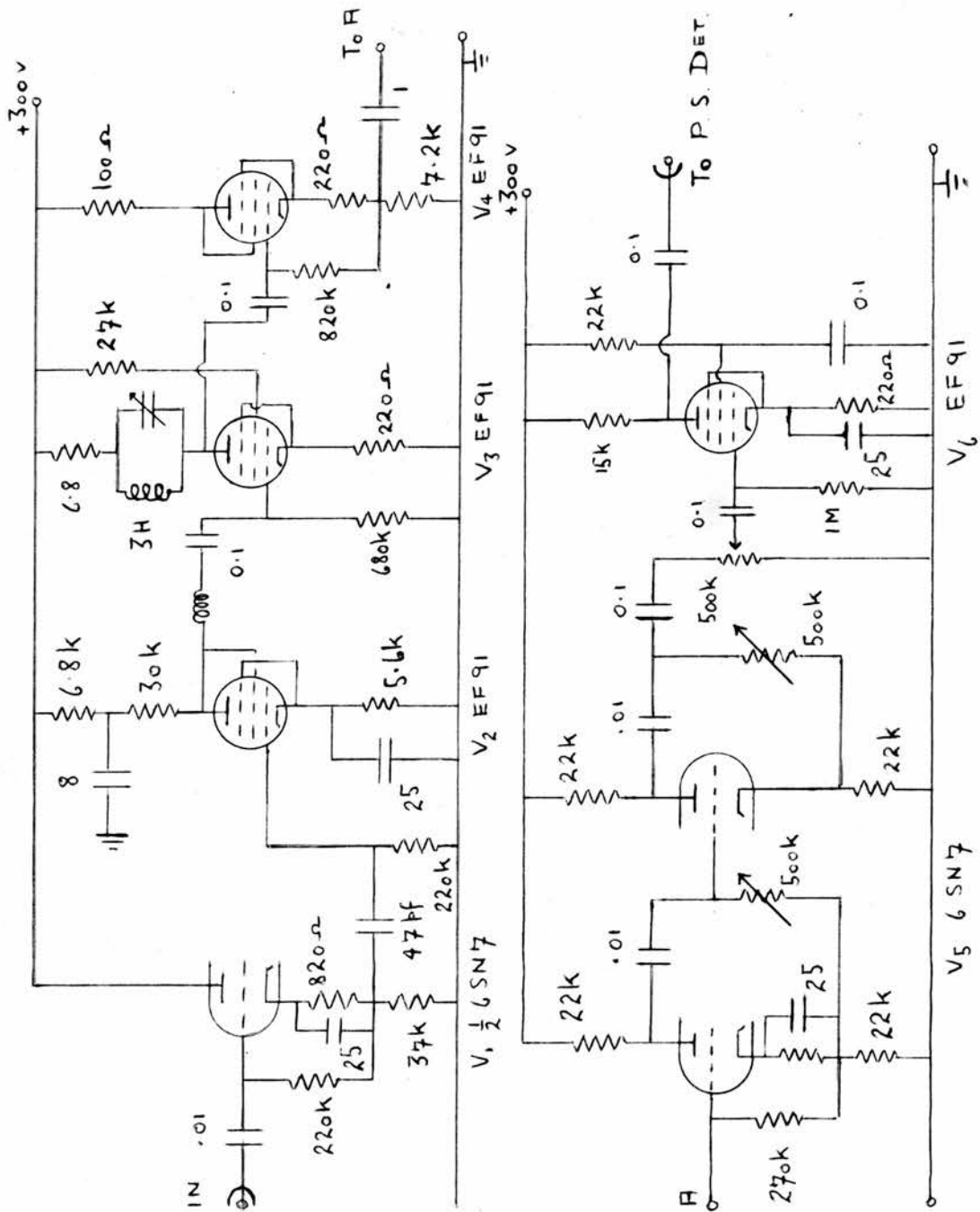


Fig. No. 26.
N.B. Amplifier II.

$$\left(\frac{V}{V_r}\right)^2 = \frac{1}{1 + 4a^2}$$

where

$$a = Q \cdot \frac{v - v_0}{v_0}$$

If now, the sweep width is very small compared with the width of the resonance curve, the amplitude modulation of the R.F. carrier as given by Fig.17.f is equal to the modulus of the derivative of the resonance curve.

$$\text{i.e. } \left| \frac{d(V/V_r)}{dv} \right| = [1 + 4a^2]^{-3/2} \frac{4Qa}{v_0}$$

for small a (i.e. in the vicinity of v_0)

$$\left| \frac{d(V/V_r)}{dv} \right| = + \frac{4aQ}{v_0} \quad (6)$$

From Schuster³⁷ the current in the anode loads of the gating valves V_2, V_3 (Fig.24) for a signal e_g is approximately

$$i = g_m e_g$$

g_m is the mutual conductance of the signal input valve V_1 so that the voltage V_a developed across the anodes is

$$V_a = R_L g_m e_g$$

$$\therefore \frac{dV_a}{dv} = R_L g_m \frac{de_g}{dv}$$

The signal input e_g to the detector is equal to the gain G of the narrow band amplifier times the amplitude

modulation of the R.F. carrier e_i

$$e_g = G e_i$$

$$\therefore \frac{dV_a}{dv} = R_L g_m G \frac{de_i}{dv}$$

but from equation 6

$$\frac{de_i}{dv} = V_r \frac{d}{dv} \left(\frac{d(V/V_r)}{dv} \right) = V_r \frac{4Q^2}{v_0^2}$$

$$\therefore \frac{dV_a}{dv} = R_L g_m G \frac{4V_r Q^2}{v_0^2} \quad (7)$$

The minimum value of V_a is that voltage which will cause a detectable current " i_G " to flow through the output micro-ammeter. Taking the resistance of the meter as R_G gives

$$V_a(\min) = i_G R_G$$

or

$$dv \geq \frac{i_G R_G v_0^2}{4 R_L g_m G V_r Q^2} \quad (8)$$

Substitution of the relevant values reveals that, under ideal working conditions, the minimum detectable signal is equivalent to a frequency change of < 1 cycle/second near the resonance value of frequency.

The final equation, shows the importance of having a Q value as large as possible. The sensitivity derived above can be increased by a factor of ten by considering

a finite sweep width, which gives a larger value of modulation amplitude at any point on the derivative curve. The resultant distortion of the derivative curve is unimportant in this case, as only a value of resonance frequency is required.

An estimate of sensitivity based on the actual value of the output voltage of the N.B. amplifier shows that the sensitivity required, i.e. ± 5 c/s off resonance (section II.II.3) can be achieved if this voltage is equal to 20 volts r.m.s. at the inversion peaks.

IV.III "Setting-up" procedure

The setting-up procedure proved to be the limiting factor in determining the accuracy of the resonance detection for although the system is sufficiently sensitive to detect small frequency changes (\sim few cycles), it was found that two consecutive readings of the resonance frequency could differ by as much as $2-3 \times 10^3$ c/s. The trouble lies in the fact that the signal from the N.B. amplifier suffers a gradual phase change of 180° between the inversion peaks, i.e. if the system is not properly aligned, a zero reading can be obtained on the detector meter even when there is a signal present, if this signal is 90° out of phase with the reference voltage.

Influenced by this anomaly, it was decided that the best approach to the problem would be to detect resonance by the phase shift rather than by trying to find the correct zero signal. The principle being that if the signal and reference to the P.S. detector are exactly in phase at the inversion peaks, then at resonance, because of the 90° phase change, there will be no deflection of the meter reading.

Several methods, such as using pulsed wave forms, were tried to ensure the correct phase relationship and the best (most reproducible) results were obtained with the following procedure, which involves the use of a high frequency signal generator and an auxiliary two stage amplifier (Fig.12).

A low frequency signal, derived from the amplitude modulation on the R.F. carrier from the signal generator, is fed from the N.B. amplifier to the auxiliary amplifier. This signal is fed directly to the signal input of the P.S. detector and also through the amplifier to the reference input of the detector. As the two stages of the amplifier introduce a 180° phase shift between the "signal" and "signal as reference", they bear the correct phase relationship for optimum deflection of the meter. An inversion peak is found by tuning the signal generator to give maximum deflection of the meter. The reference input is then

switched to the correct reference signal from the frequency doubler, and the signal phase altered to give once again a maximum deflection of the detector meter. At this point, it is known that the signal and reference are exactly in phase at the inversion peak. The complete switching sequence is given in section IV.V.1

IV.IV D.C. Magnetisation

While still carrying out room temperature tests on the detection system, it was noticed that the resonant frequency of the tank circuit tended to drift at rates ranging from 6 cycles/minute to about 100 cycles/minute. A probable cause of this effect was thought to be a varying D.C. magnetisation of the ferrite core. This would alter the permeability of the core and hence cause a slow variation of the tank circuit inductance L . A check showed that there was a D.C. magnetisation of the core.

The first step taken to eliminate this effect was to remove the penning gauge head from the top plate, as it was found that the stray magnetic field from the gauge magnet was relatively strong in the vicinity of the ferrite core. This was not completely successful, but reduced the drift to the lower level quoted above. Further investigation indicated that the drift rate was highest

immediately after switching on the L.F. oscillator. This was again thought to be a D.C. magnetisation effect caused by surges in the sweep coil on switching on the L.F. oscillator. The fact that the drift rate diminished over a period of time (~ 4-6 hours) to about 5 cycles/minute, suggested that if the oscillator be allowed to run continuously this drift should disappear or become negligible and further that when the core is cooled to about 100°K there might be a "freezing-in" of the D.C. magnetisation completely eliminating the drift.

IV.V Low Temperature Performance

IV.V.1 Description of a Typical Run

Before starting a run, the dilatometer is precooled with liquid air to about 100°K and is then allowed to heat up slowly again to room temperature. This operation is usually performed during the 24 hours prior to starting a run, and was found necessary to obtain any degree of reproducibility in the results. Because of the temperature variation of liquid air, it is necessary to use nitrogen (or oxygen) as the coolant liquid during the actual recording part of the run. This involves siphoning off the liquid air, which is used only in the interest of economy.

Before taking readings, the electronic units are

switched on for 4-6 hours, (all the oscillators run continuously) and the alignment is carried out after this initial heating up period. The reference signal from the frequency doubler is displayed on an oscilloscope (C.R.O.) and the L.F. oscillator is tuned to the resonant frequency of the twin-T networks, giving an output voltage of the order of 100 volts peak to peak. In the same way, the N.B. amplifier is tuned to give an output signal of about 20 volts r.m.s. with the carrier from the R.F. oscillator tuned to one of the inversion peaks. The remaining preliminary setting consists in switching the carrier input to the H.F. signal generator. The resultant signal from the N.B. amplifier is then fed to the auxiliary amplifier (Fig.12) and the output of the signal generator varied so that the output of the amplifier is about 100 volts at the inversion peaks and the input about 4 volts at the same point. These initial settings need not be altered during the period of a run.

The first frequency reading is usually taken with the dilatometer close to room temperature. Normally, a period of about half an hour to an hour is required, after switching on the dilatometer heater, for the temperature to become completely stable. The frequency readings are then taken in the following way.

1. The R.F. oscillator is tuned as close to resonance as possible by display on a C.R.O. and the output of the mixer is set to within the limits 0.2-2 volts r.m.s.

2. The H.F. signal generator is tuned to one of the inversion peaks by obtaining a maximum deflection of the detector meter with the reference derived from the auxiliary amplifier and the signal straight from the N.B. amplifier (section IV.III).

3. With the same signal, but with the reference taken from the frequency doubler, the detector meter is again to a maximum deflection with the phase shifters of the N.B. amplifier.

4. With no signal, the detector is set to zero deflection with the reference from the frequency doubler.

5. With the same reference, but with the signal now derived from the carrier of the R.F. oscillator, the meter reading is set to zero by tuning the R.F. oscillator.

6. This is now "resonance", and the frequency is read on the Cintel.

7. The whole procedure is repeated several times (from (2)) to verify the frequency reading obtained.

The time required to carry out this series of steps from (2) to (6) is about 1 minute, and the time elapsing between detection of resonance and measuring the frequency

((5) - (6)) is only the time required to press the "counting switch" on the Cintel, i.e. a few seconds.

The resonant frequency drifts until temperature equilibrium is reached, and then frequency readings, obtained as above, are taken every 10 minutes until two successive readings are the same to within the required limits.

Equilibrium state readings are taken with 30° intervals, and then repeated in a second run at the intermediate temperatures, giving a check on both sets of readings and giving a set of readings at 15° intervals.

IV.V.2 Results of Runs

(a) Cryostat and Temperature Measurement System

The initial runs were used to get an indication of the efficiency of the cryostat and the temperature measurement system and to calibrate the heater on the dilatometer can. The performance of the temperature measurement system has already been discussed (section II.IV.6). So far, only nitrogen has been used as the coolant liquid and the heat losses bear a satisfactory agreement with those estimated (they are in fact 20% less).

These checks therefore showed that the cryogenic section of the apparatus operates as specified and that no modifications were required.

(b) Detection system

The expected frequency change of the resonant tank circuit, with a copper specimen, is of the order of 50 c/s per degree at room temperature, and because of areal changes of the plates, this should be a positive change (i.e. frequency increasing as temperature decreases). The first two runs gave an increasing frequency change down to $T \sim 200^{\circ}\text{K}$ and then an increasing change; the magnitude of the change being a factor of 6 greater than expected in the higher temperature regions.

This "dip" in the curve was removed by increasing the clearance between the distance piece of the specimen holder (E) and the barrel of the dilatometer (Fig.2). This discrepancy was presumably caused by the fact that the three retaining springs (B') were not sufficiently strong to hold the specimen holder in position against the shoulder of the barrel, when a gap occurred due to thermal gradients in the cooling process.

The following two runs gave exactly similar curves, but instead of a positive frequency change, the results showed a negative change of $\sim 2 \times 10^3$ c/s per degree at room temperature. Because of the constancy of these two sets of results, it was decided to replace the copper specimen with a diamond specimen to see if the frequency

change was caused by a separation of the condenser plates or by some spurious effect in another part of the cryostat, which was masking the change looked for.

From the results obtained with the diamond, it was possible to estimate the expansion coefficient of copper by assuming a negligible expansion coefficient for the diamond. Thus, the frequency change obtained with the diamond specimen would be equivalent to that caused by the length change of an equivalent length of copper. As a rough check, it was assumed that the results obtained from the copper run were a zero effect and that direct subtraction of the two curves would give the expansion coefficient of copper. This was found to be correct, i.e. the result calculated for copper gave the correct order of magnitude. This was taken to imply that the large frequency changes found from the copper run were, in fact, caused by an increase in gap of the dilatometer condenser.

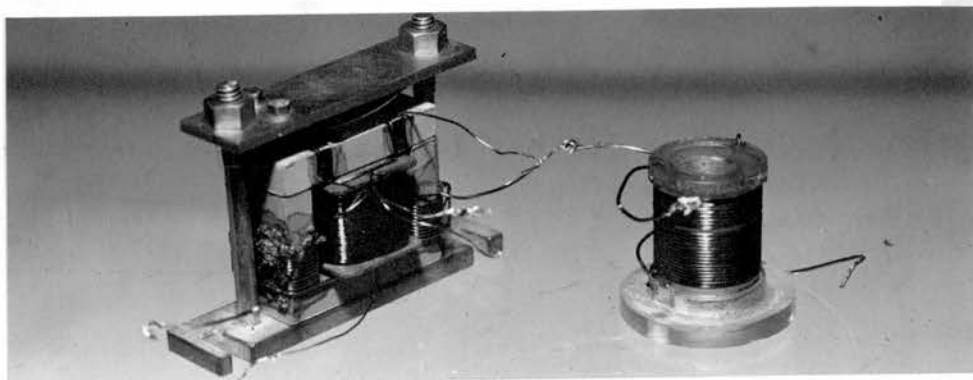
The cause of this, when found, appeared particularly obvious and was removed, as shown in the photo of Fig.3.a, by soldering a flat spiral of wire between the top plate of the dilatometer condenser and the connection to the inductance, through the copper glass seal (Fig.7.b). Initially, this connection was made directly with a straight piece of wire and when the dilatometer was cooled, the

differential contraction between the glass of the seal and the copper wire resulted in the top plate of the condenser being raised relative to the membrane against the force of the three small retaining springs, B. (Fig.2).

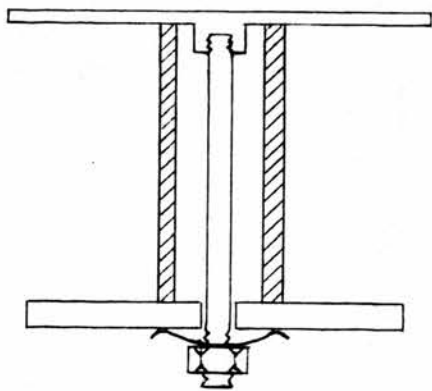
This small change had the desired effect, (i.e. elimination of the large frequency changes) but also resulted in a major modification in specimen shape, because of the inadequacy of the phosphor bronze membrane. It was found that the large frequency changes were masking a much smaller effect probably caused by buckling of the membrane. This was inferred from the fact that succeeding runs gave a positive frequency change of the correct order of magnitude but that there was a large degree of scatter in the plotted points, and that these were not reproducible.

A mushroom shaped bottom plate for the condenser was made and positioned in the specimen holder as shown in Fig. 27.b. It was found, however, that although the results of each separate run, with the mushroom specimen holder, gave a smooth curve, the slope of each of these curves, although of the correct order of magnitude, varied from run to run and could have been caused only by a change in characteristics of the ferrite core.

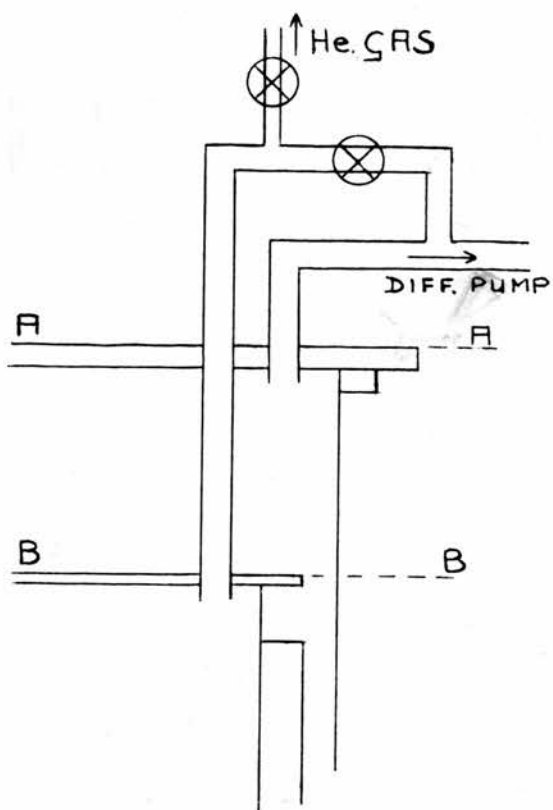
It seems, therefore, that although the use of ferrite cores is in principle very sound, their application to



(a)



(b)



(c)

Fig. No. 27.
Modifications.

problems of this nature is rather hazardous.

Lack of time made further low temperature investigation impossible, but a room temperature trial with a vibrating reed condenser indicated that this approach could probably be pursued quite profitably once minor difficulties are overcome.

An immediate advantage of not using a ferrite is the increase in Q value which can be obtained with an air cored inductance. As seen from equation 8, this would give a marked increase in sensitivity of the detection system.

IV.VI Conclusions and recommendations

Although the apparatus has not been sufficiently developed to obtain final results, the work described in this thesis indicates that the principle is basically sound. The performance of the cryogenic section of the apparatus is as originally required but it is felt that the dilatometer could be profitably reduced in weight, thereby substantially diminishing the cooling times.

The electronics section, especially the detection system, proved much more troublesome than anticipated, both in design and construction. The sensitivity of detection, however, achieved with the ferrite cores is at least as great as that required, but as pointed out in section IV.V.2, the system is not really practicable. Use of a

vibrating reed condenser should overcome the defects of the ferrite cores, but unfortunately will also result in a loss of sensitivity by a factor $C/(C + C_v)$ where C is the capacity of the dilatometer condenser and C_v is the mean capacity of the vibrating reed condenser.

The overall sensitivity of the present system could be increased by using a higher frequency for the carrier wave. This, however, would raise the difficulty of frequency measurement which must be as accurate as the sensitivity of detection. Another important point noted in section II.II.3 is that the sensitivity of detection in practice is less than the ideal calculated value by $C/(C + C_e)$, where C_e is the stray earth capacity in the dilatometer tank circuit. If $C_e \ll C$, this effect is negligible, but it might be completely eliminated by employing a three terminal capacitor as used by White¹² in his experiments on thermal expansion.

When certain crystal diodes are subject to a D.C. bias in the negative direction, they exhibit a capacitance effect across the terminals which is dependent on the magnitude of the applied voltage. These are called back bias diodes, and give a capacity of a few pico farads with a potential of the order of 5-10 volts. This effect could probably be utilised in one of the following ways.

(1) Automatic Frequency Control

The output of the phase sensitive detector is either a positive or negative D.C. voltage, depending on whether the R.F. oscillator frequency is greater or smaller than that required for resonance. It would be possible to lock the frequency of the oscillator to the resonant frequency of the dilatometer L.C. circuit if it were possible to feed the output of the detector to some control element in the oscillator tank circuit. A crystal diode, suitably biased, in parallel with the capacitive element of the oscillator tank circuit would fill this requirement in that, should the oscillator frequency, initially tuned to resonance, drift slightly, the resultant D.C. output of the P.S. detector fed back to the diode would bring the frequency back to the initial value.

The degree of frequency control would be dependent on the "Q" of the dilatometer L.C. circuit. The low Q obtained with the ferrite cored inductance could be vastly improved with an air cored inductance using a vibrating reed condenser to supply the sweep for amplitude modulation of the carrier signal.

(2) Frequency sweep

As stated in section III.III.1, an amplitude modulated pick-up signal could be obtained, if the input from the

R.F. oscillator is suitably frequency modulated and resonance detected as before. This effect could be obtained by placing the diode as above in parallel with the capacitive element of the oscillator tank circuit and applying a L.F. sweep voltage. The main difficulty envisaged with this scheme would be in measuring the resonant frequency. To do this, it would be necessary to "switch off" the sweep voltage and to ensure, in some way, that the D.C. back bias is exactly the same after switching off as it was while detecting the resonant frequency of the dilatometer L.C. circuit.

The very great advantage of this method is that the characteristics of the dilatometer L.C. circuit would remain substantially unaltered from one run to the next.

(3) Additional capacity in dilatometer tank circuit

The difficulty of the frequency sweep method could be overcome by using the diode as the "modulating element" in the dilatometer tank circuit instead of either a vibrating reed condenser or a ferrite cored inductance. This method is probably the least likely to apply, because two major snags immediately arise. The first is in not only maintaining a constant negative bias for the period of a run and so obtaining a constant value of capacity, but also in ensuring the same value in consecutive runs. Assuming

this could be overcome using a potentiometer or similar control, there is no reason to expect that the diode will retain its properties and characteristics after repeated coolings to low temperatures. Only an extensive trial would indicate if the application of diodes is a feasible proposition.

The cooling curves of Fig.9.a show that the fastest cooling rates can be obtained by allowing a few m.m. of helium gas into the outer can; the objection to this method of cooling being the conduction losses from the liquid air can. A simple modification in cryostat design could have made this method practicable. By making the radiation shield vacuum tight (small leaks would not matter) it would be possible as shown in Fig.27.c to isolate the volume inside the radiation shield and allow in helium exchange gas for the cooling process to liquid air temperatures, while keeping the outer can pumped. The upper heat switch could then be dispensed with and the system made much more efficient.

REFERENCES

1. Mie, Ann.d.Physik, 11, 657, 1903.
2. Grüneisen, Handbuch d.Physik, 10, 1, 1926.
3. Slater, "Introd. to Chemical Physics", McGraw-Hill, p.234.
4. Kittel, "Solid State Physics", Wiley, p.152.
5. Bijl and Pullan, Phil.Mag., 45, 290, 1954.
6. As 3, p.240.
7. Bijl and Pullan, Physica, 21, 285, 1955.
8. Barron, Phil.Mag., 46, 720, 1955.
9. Simmons and Balluffi, Phys.Rev., 108, 278, 1957.
10. Rubin et al., J.Am.Chem.Soc., 76, 5289, 1954.
11. Dheer et al., Phil.Mag., 3, 665, 1958.
12. White, Cryogenics, 1, 151, 1961; Nature, 187, 927, 1960.
13. Abbis et al., 7th International Conference on L.T. Physics
Fraser et al. - Toronto, 1960.
14. Horton, Can.J.Phys., 39, 263, 1961.
15. Visvanathan, Phs.Rev., 81, 626, 1951.
16. Ruhemann, Low Temperature Physics, (Cambridge), 1937.
17. Jacobs and Goetz, Phys.Rev., 51, 159, 1937.
18. Hume-Rothery, Proc.Phys.Soc., 51, 209, 1945.
19. Fizean, Pogg.Ann., 128, 564, 1866.
20. Vernon and Weintraub, Proc.Phys.Soc., 66, 887, 1953.
21. Staker, Phys.Rev., 61, 653, 1942.
22. Michels et al., Physica, 19, 371, 1953.

REFERENCES

23. Huzan et al., Phil.Mag., 6, 277, 1961.
24. Jones, Proc.Phys.Soc., 71, 280, 1958.
25. Lilly, Rev.Sci.Inst., 13, 34, 1942.
26. Willey, J.Sci.Inst., 23, 264, 1946.
27. Manchester, Can.J.Physics, 37, 989, 1959.
28. MacDonald, J.Sci.Inst., 24, 232, 1947.
29. Clapp, Proc.I.R.E., 36, 356, 1948.
30. Terman, "Radio Engineer's Handbook", McGraw-Hill, p.485.
31. Meachem, Proc.I.R.E., 26, 1278, 1938.
32. Terman, as 30, p.492.
33. Scott, "The Physics of Electricity and Magnetism", Wiley p.364.
34. Edson, "Vacuum Tube Oscillators", Wiley and Sons, p.138.
35. Valley and Wallman, "M.I.T. Radiation Lab.Series", Vol. 18, p.384.
36. Ettinger, "Magnetic Amplifiers", Methven, p.6.
37. Schuster, Rev.Sci.Inst., 22, 254, 1951.
38. Parker, "Electronics", Arnold, p.374.

ACKNOWLEDGEMENTS

I should like to record my sincere thanks to:-

- Professor J. F. Allen, F.R.S. : for allowing me the facilities of Edgecliffe Research Laboratory.
- Dr D. Bijl, F.R.S.E. : for suggesting the topic and his supervision.
- Mr J. Gerrard : for the photography and printing of the drawings.
- Messrs J. McNab, M. Bird,
G. Dunsire and
F. Akerboom : for constructing the cryogenic section of the apparatus.
- Mr R. Mitchell : for an ever-ready supply of liquid coolants.
- Mr A. M. Ironside, B.Sc. : for his help in conducting the experimental runs.
- Miss J. M. Lawson : for her efficient and rapid typing of the thesis.
- The Department of Scientific and Industrial Research : for the award of a maintenance grant.